land

MDPI

Article

Identification and Prediction of Land Use Spatial Conflicts in Urban Agglomeration on the Northern Slope of Tianshan Mountains Under the Background of Urbanization

Yunfei Ma [1,2], Yusuyunjiang Mamitimin [1,2,*] and Ailijiang Nuerla [3]

[1] College of Geography and Remote Sensing Sciences, Xinjiang University, Urumqi 830017, China; grmayunfei@163.com
[2] Key Laboratory of Smart City and Environment Modeling of Higher Education Institute, Urumqi 830017, China
[3] College of Ecology and Environment, Xinjiang University, Urumqi 830017, China; aljnel@xju.edu.cn
* Correspondence: y.mamitimin@xju.edu.cn; Tel.: +86-152-768-62217

Abstract: In past decades, urbanization has entered a phase of rapid development, resulting in an intensified utilization of land resources. The finite nature of these resources has led to increased pressure on land availability, giving rise to a phenomenon known as land use conflict. This conflict is particularly evident in the frequent conversion of land categories, with urban impervious surfaces increasingly encroaching upon forests, grasslands, and agricultural land. Such encroachments trigger a series of land use conflict issues, which subsequently impact the function and structure of regional ecosystems. This paper analyzes the spatial and temporal changes in land use and land cover (LULC) within the urban agglomeration on the northern slope of Tianshan Mountain. It measures and evaluates the spatial and temporal evolution of land use conflicts in the study area from 1990 to 2020, utilizing conflict-related theories and the landscape risk evaluation model. Additionally, the paper explores the spatial and temporal dimensions of land use conflicts under three scenarios—natural development (ND), cultivation priority (CP), and ecological priority (EP)—for the years 2030 and 2050, informed by the Future Land Use Simulation (FLUS) model. The results indicate that unused land constitutes the predominant land use type, accounting for over 50% of the total area. The areas of cultivated land, water bodies, and urban land are experiencing an increasing trend, while the areas of forestland, grassland, and unused land are witnessing a decreasing trend. The level of land use spatial conflicts during the study period showed a decreasing and then increasing trend, with an overall upward trend and an increase in the average value of 0.03. In terms of the proportion of spatial units, mild and general conflicts exhibited a decreasing trend, with reductions of 4.21% and 2.95%, respectively. Conversely, the proportion of medium conflicts increased significantly, rising by 7.33%, while severe conflicts experienced a slight increase of 0.23%. Under the ND, CP, and EP scenarios, the spatial and temporal dynamics of future land use conflicts varied. However, the study area was predominantly characterized by general conflicts in both 2030 and 2050. In 2030, the proportions of spatial units experiencing general conflicts in the three scenarios are projected to be 61.20%, 60.39%, and 57.51%, respectively. In comparison, these proportions are projected to be 59.24%, 62.70%, and 56.29% in 2050, respectively. The anticipated future changes in land use spatial conflicts vary across different scenarios. Notably, the ND scenario indicates a rising conflict level in the study area over the next 30 years, with an overall increase of 0.03 in the mean value. In contrast, the changes in the index under the CP and EP scenarios are relatively stable.

check for updates

Academic Editor: Tao Liu

Received: 18 November 2024
Revised: 20 January 2025
Accepted: 21 January 2025
Published: 22 January 2025

Citation: Ma, Y.; Mamitimin, Y.; Nuerla, A. Identification and Prediction of Land Use Spatial Conflicts in Urban Agglomeration on the Northern Slope of Tianshan Mountains Under the Background of Urbanization. *Land* **2025**, *14*, 228. https://doi.org/10.3390/land14020228

Copyright: © 2025 by the authors. Licensee MDPI, Basel, Switzerland. This article is an open access article distributed under the terms and conditions of the Creative Commons Attribution (CC BY) license (https://creativecommons.org/licenses/by/4.0/).

Keywords: land use; spatial conflict; landscape pattern; spatiotemporal evolution; FLUS model

1. Introduction

The limited nature of land resources and the negative externalities of land resources have led to increasingly significant land use conflicts [1]. Land use spatial conflict primarily revolves around the competition for the same geographical area of land resources. It involves the interests of various parties engaging in competition over time, space, and strategic considerations. Land use conflict can be understood as the differences and inconsistencies that arise among the parties involved in land resource utilization. This conflict encompasses not only the various methods of land use but also the environmental conflicts that may arise [2]. This conflict reflects competing interests and the changing functions of diverse land uses [3]. A city cluster is a high-level spatial configuration of an urban system, characterized by the aggregation of several geographically proximate cities that are interconnected across various economic and social dimensions [4]. In the process of urbanization, spatial changes in land use are mainly reflected through the gradual advancement of neighborhoods and the outward expansion of cities [5]. Recently, the rapid advancement of urbanization has resulted in a significant increase in the demand for spatial resource development and utilization [6–8]. Consequently, regional ecosystems have experienced damage, leading to disorganized functions. This is particularly evident during land reclamation and the expansion of urban construction, where many high-quality spatial resources have been destroyed. Such degradation has further exacerbated a variety of conflicts and contradictions [9–11]. Therefore, carrying out the identification and prediction of spatial conflicts in land use can provide a theoretical basis for the optimal use and allocation of land resources, better realize the coordinated development of land use, and promote the sustainable development of regional economy and society.

Land use spatial conflict refers to the disputes arising among various resource users during the development and utilization of land resources, driven by the pursuit of personal interests [12,13], and such conflicts can result in negative impacts at three levels: social, economic, and ecological [14–16]. In the 1980s, research on land use conflicts began to gain international attention. The causes of these conflicts can be categorized into intrinsic and extrinsic factors [17]. Currently, numerous foreign scholars have examined the causes of land use conflicts. Intrinsic factors emphasize the scarcity of land resources, such as Campbell and others, based on the relationship between animal husbandry, agricultural farming, and wildlife conservation, pointing out that land use conflict is the competition and contradiction caused by different types of land development and utilization due to the scarcity of land [17]; Moore and others have argued that the fixed geographic location of land is also key to conflict [18]. External factors focus on the conflicts between land use subjects due to the competition for rights and interests, such as socioeconomic development, population growth, and urban planning, etc. Benjaminsen et al. argue that land regulations and socioeconomic benefits are external factors contributing to contradictions in land use conflicts [19]. In contrast, Tudor et al. contend that land use conflicts arise from environmental and social issues stemming from the aggregation of various land use stakeholders [20]. Research on the spatial conflict of land use encompasses various aspects, including landscape patterns, ecological environmental protection, sustainable development, and socioeconomics. Additionally, the methodologies employed in this field are diverse and well-developed. In 2004, Sauer employed two distinct spatial scales to thoroughly investigate the factors contributing to conflict formation among various

stakeholders in both a coastal tourism area and an agricultural region [21]. In the same year, Cristian utilized a multicriteria analysis to assess land use conflicts in the Bucharest region [22]. In 2016, Valera C. A. analyzed land use conflicts in the state of Minas Gerais, Brazil, from an ecological perspective [23]. Meanwhile, Hunsberger and other scholars employed Geographic Information Systems (GISs) as a tool to study the relationship between land use conflicts and climate change in Cambodia [24].

With the growing emphasis on land use conflicts, domestic scholars have incorporated empirical observations to analyze these conflicts across three dimensions, namely the subjects and objects involved, as well as the external environment. As for the object of conflict, that is, the land resource itself, some studies have pointed out that the scarcity of land resources and its fixed location nature exacerbate the contradiction between the supply and demand of land, which is unable to satisfy the needs of the country's population growth and socioeconomic development [25], and, furthermore, the multifunctionality and value diversity of the land in the process of its use may lead to conflicts among stakeholders in the pursuit of different values [26]. From the perspective of the subject of the conflict, that is, the land use participants, conflicts are triggered by disagreements among parties, including landowners, users, and managers, over land use adjustment, revenue distribution, and development and utilization. Ma et al. argue that participants in the land use process exhibit inconsistencies across various aspects, including land use adjustments, land revenue, and development and utilization. These inconsistencies contribute to the emergence of land use conflicts [27]. External environmental factors, such as differences in government planning philosophies, are also included in the causes of conflict, and are an important factor in land use conflicts. Leng et al. emphasize the role of government planning philosophy in generating conflict from a game theory perspective [28]. Zhou et al. analyze and measure the intensity and characteristics of land use conflicts in urban agglomerations by constructing a composite index [2]. Lv et al. evaluated land use conflicts in Jinghe County by developing a pressure–state–response (PSR) model with sub-indexes, and they also examined the spatial heterogeneity of land use conflicts, classifying hot and cold zones using a global autocorrelation index [29]. Utilizing the theory of landscape ecological risk assessment, Dai et al. measured the intensity of land use conflicts in Jiangjin District, located in the southwestern Chongqing Municipality, and employed Geoda software to reveal the overall distribution characteristics of land use conflict levels in the study area [30]. Additionally, Liao et al. constructed a conflict model of the three life spaces on Pingtan Island based on landscape patterns, demonstrating that the conflict intensity of the ecological production space was predominant during the study period [31].

Land use change can reflect the interaction between humans and the natural environment while reflecting changes in surface spatial patterns and landscapes [32,33]. The primary focus of land use research encompasses the spatial and temporal evolution characteristics, ecological effects, driving factors, and various modeling approaches. Currently, the commonly utilized prediction models include the gray prediction model, logistic regression model, cellular automata (CA), and the CLUE-S model, among others [34–37]. The FLUS model is an emerging framework developed in recent years, proposed by Liu Xiaoping's team in 2017. It comprises two modules: one based on an adaptive probabilistic computational artificial neural network (ANN), and the other on adaptive inertia cellular automata (CA). Compared to traditional land use prediction models, the FLUS model optimizes the CA component, effectively addressing the complexity and uncertainty associated with the interactions between different land use types, thereby enhancing simulation accuracy [38–40]. Currently, research utilizing the FLUS model primarily concentrates on China. Chinese scholars have successfully simulated various aspects, including carbon

emissions, land use, and "Production-Living- Ecological" space, through the FLUS model. Sun et al. utilized the FLUS model to simulate future land use changes in Longgang District, Shenzhen [41]. Similarly, Zhao et al. employed the FLUS model to project LULC changes in the Pearl River Delta at 10-year intervals for the years 2025, 2035, and 2045 [42]. Additionally, Wang et al. simulated the land use pattern of Jingtai County, Gansu Province, for the year 2030 using the FLUS model [43]. Furthermore, with the assistance of the FLUS model, Yang et al. constructed a framework for analyzing land use structure changes in the Fuling River Basin for 2030 under four different scenarios, while also simulating the evolution of its ecosystem service value [44].

Existing studies indicate that most current research on land use conflict in China primarily focuses on analyzing past conflicts, with insufficient attention given to predicting the evolution of future conflicts. Furthermore, the majority of related research has been concentrated in economically developed regions, while there is a notable lack of studies in the less economically developed and ecologically fragile areas of northwest China. This study aims to analyze the land use dynamics of the urban agglomeration on the northern slope of the Tianshan Mountains, focusing on the temporal and spatial changes in land use from 1990 to 2020. We will employ landscape pattern analysis to establish a land use conflict index assessment model, which will evaluate and classify the degree of spatial conflict in land use within this urban agglomeration during the same period. Furthermore, we will utilize the FLUS model to predict the land use spatial patterns for the years 2030 and 2050 under various scenarios. Additionally, we will apply a comprehensive measurement model for spatial conflict to assess the level of spatial conflict by simulating the land use prediction data for 2030 and 2050 obtained from the FLUS model. Based on these analyses, we will propose regulatory measures aimed at alleviating land use conflicts in the urban agglomeration on the northern slope of the Tianshan Mountains, thereby providing a scientific basis for the rational allocation of land resources and the standardization of spatial patterns.

2. Materials and Methods

2.1. Study Area

Figure 1 shows the urban agglomeration situated on the northern slopes of the Tianshan Mountains is strategically located at the center of the Asian–European continent, with geographic coordinates ranging from 83°24′ to 91°54′ E and from 41°11′ to 46°18′ N [45]. The study area is situated in the southern region of the Junggar Basin and the central part of the northern slope of the Tianshan Mountain, representing a typical "mountain–basin system" within the arid zone of Northwest China [46]. It is bordered to the north by the Gurbantunggut Desert, to the west by Jinghe County of the Bortala Mongol Autonomous Prefecture, and to the east by Balikun Hasake Autonomous County of Hami City, with an average elevation of 1000 m above sea level. This urban agglomeration entirely encompasses the cities of Urumqi, Changji Hui Autonomous Prefecture, Turpan, and Karamay, along with the city of Kuitun in Ili Prefecture, the city of Wusu, and the county of Shawan in Tacheng Prefecture. Additionally, it includes the municipalities of the Corps within the planning area, covering a total area of 215,400 square kilometers. The study area is situated in the typical arid zone of Northwest China, characterized by an arid continental climate. It experiences an average annual temperature of 7.4 °C, with an average annual precipitation of 215 mm and an average annual evapotranspiration of 1825 mm [47]. The distribution of precipitation exhibits significant spatial variability, decreasing from south to north. Precipitation levels range from 220 mm in the southern regions to 100 mm in the northern areas, with approximately 70% of the total precipitation occurring during the rainy season, which spans from June to September [48]. The region slopes gently from southeast

to northwest and spans a variety of landform types, including mountains, alluvial flood fans, flood plains, lakes, and deserts [48]. The scarcity of water resources constrains the region's economic development, with the primary sources of water for both production and domestic use being the meltwater from alpine snow and ice, as well as surface water from the Urumqi, Manas, and Kuitun rivers [47]. The study area is extensive, sparsely populated, and characterized by a diverse mix of ethnic groups. By the end of 2018, the population of the urban agglomeration reached 5,917,100, which constituted approximately one-fifth of the population of the autonomous region. Among this population, 4,898,600 individuals were urbanized, representing 42.25% of Xinjiang's urbanized population. Additionally, the region's GDP was recorded at 6566.45 $\times$ 10^8 RMB, accounting for about half of Xinjiang's total GDP. Currently, this area is recognized as Xinjiang's most advanced region in terms of economic development, transportation networks, population density, and industrial activity. The region is situated in northern Xinjiang, at the heart of the Silk Road Economic Belt. It is one of the 19 urban agglomerations prioritized by China in the 14th Five-Year Plan and is one of the two border urban agglomerations specifically targeted for development. Notably, it is the only urban agglomeration established in the core area of the Silk Road Economic Belt. As a key area for Xinjiang's economic and social development, its strategic location is of utmost importance [49].

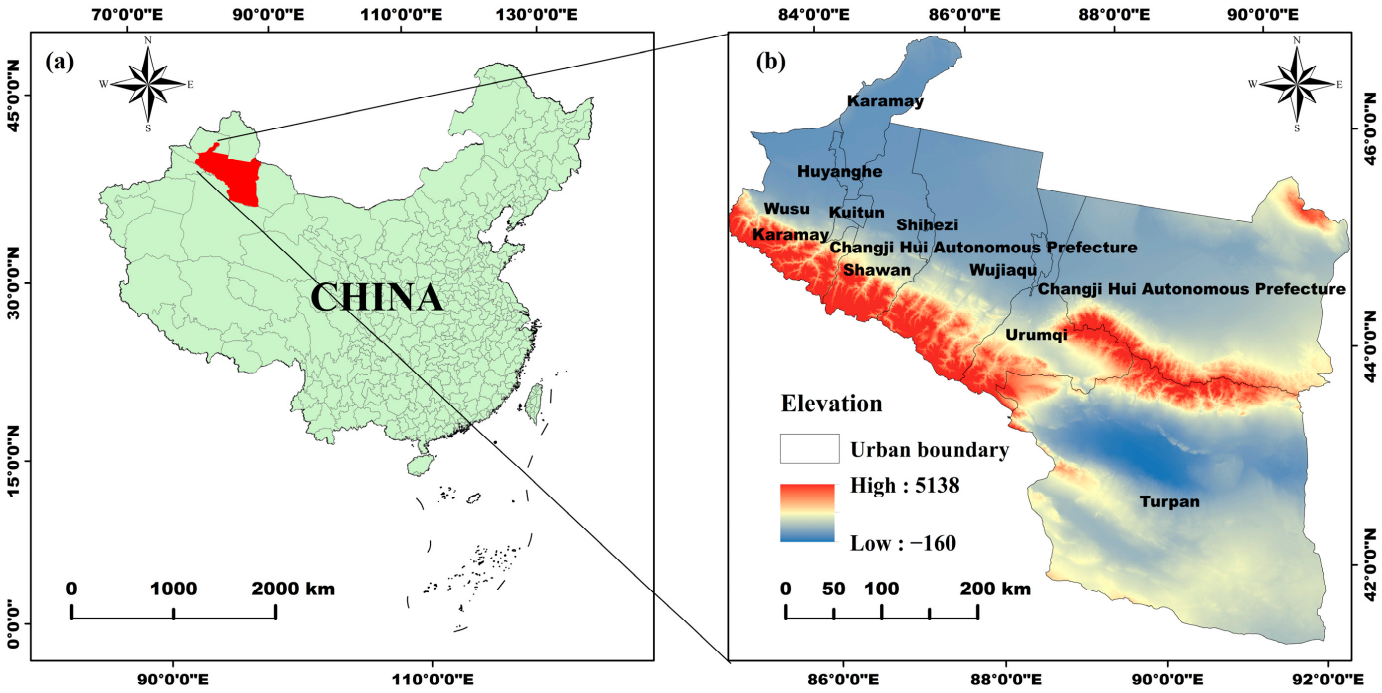

Figure 1. Geographical location (**a**) and topographic map (**b**) of the study area.

2.2. Data Sources

The land use data utilized in this study were sourced from the Resource and Environment Science Data Center of the Chinese Academy of Sciences (https://www.resdc.cn, accessed on 16 November 2024) and possess a spatial resolution of 30 m. The land use data for the study area were derived using the cropping function in ArcGIS. Digital Elevation Model (DEM) data were obtained from the Geospatial Data Cloud (https://www.gscloud.cn, accessed on 16 November 2024), also with an initial spatial resolution of 30 m, from which slope and slope direction data were calculated. Annual precipitation, mean annual temperature, and the Normalized Difference Vegetation Index (NDVI) were acquired from the Resource and Environment Science Data Center of the Chinese Academy of Sciences

(https://www.resdc.cn, accessed on 16 November 2024) at an initial resolution of 1 km. Road and settlement data were sourced from OpenStreetMap (https://openmaptiles.org, accessed on 16 November 2024). Additionally, gross domestic product (GDP) and population data were obtained from GitHub (https://github.com, accessed on 16 November 2024) and LandScan (https://landscan.ornl.gov, accessed on 16 November 2024), respectively, both at a resolution of 1 km.

2.3. Data Processing

2.3.1. Analysis of Changes in LULC

The formula for calculating the magnitude of area change in LULC is as follows:

$$R = \frac{U_2 - U_1}{U_1} \times 100\% \quad (1)$$

where U_1 and U_2 are the area of a land class in the starting year of the study and the final period of the study, respectively, and R represents the magnitude of change in the area of a land class over a given time period [50].

2.3.2. Land Use Spatial Conflict Evaluation Model

This paper develops a metric model of land use spatial conflicts based on landscape patterns, utilizing the "risk source + risk receptor—risk effect" framework from landscape ecological risk evaluation methods and related studies [31,51–53]. The formula for calculating the spatial conflict of land use is presented as follows:

$$LUCI = CI + FI - SI \quad (2)$$

where the Land Use Conflict Index (*LUCI*) corresponds to the degree of landscape risk level, here denoted as the land use spatial conflict composite index; *CI*, *FI*, and *SI* correspond to regional ecological risk sources, risk receptors, and risk effects, respectively, and are denoted here as the spatial Complexity Index (*CI*), spatial Fragility Index (*FI*) and spatial Stability Index (*SI*).

The *CI* characterizes the extent to which neighboring landscapes influence the current LULC [51]. In the field of landscape ecology, the area-weighted mean patch fractional dimension (*AWMPFD*) is positively correlated with the complexity of landscape patch boundaries, indicating a greater likelihood that a patch will be affected by its neighbors. In this paper, the *AWMPFD* index is employed as a substitute for *CI* [51], as in the following Equation (3):

$$AWMPFD = \sum_{i=1}^{m} \sum_{j=1}^{n} \left[\frac{2ln(0.25P_{ij})}{ln(a_{ij})} \left(\frac{a_{ij}}{A} \right) \right] \quad (3)$$

where P_{ij} is the perimeter of the patch, α_{aj} is the area of the patch, A is the total area of the spatial unit, m is the total number of evaluation units in the study area, and n is the number of trichotomous spatial types.

FI is indicative of the inherent attributes of the risk receptor and is closely linked to the characteristics of the land use itself. It primarily delineates the vulnerability traits exhibited by the land use system in response to external pressures, reflecting the sensitivity of various landscape types to external disturbances. Research has demonstrated that a higher *FI* correlates with a weaker land use structure in the face of disturbances, increased vulnerability of the landscape to external environmental influences, and heightened intensity of land use conflicts [31,51–53]. Equation (4) is as follows:

$$FI = \sum_{i=1}^{n} F_i \times \frac{a_i}{S} (n = 6) \quad (4)$$

where F_i is the fragility index of each type of landscape; α_i is the area of each type of landscape in each unit; and S is the total area of the spatial unit. Referring to the existing research results and the status quo of the study area, the values were assigned to six landscape types [53], from low to high, as follows: urban land = 1, forestland = 2, grassland = 3, cultivated land = 4, water bodies = 5, and unused land = 6. After normalization, the F_i values of the urban land, forestland, grassland, cultivated land, water bodies, and unused land were 0.047619048, 0.095238095, 0.142857143, 0.19047619, 0.095238095, 0.142857143, 0.19047619, 0.238095238, and 0.285714286, respectively.

SI refers to the phenomenon in which landscape patches become fragmented due to the impact of external pressures on geospatial structures, thereby reflecting the stability of spatial units [54]. This index is used to indicate stability [2], and patch density is positively correlated with landscape fragmentation within the region and the likelihood of land resources being exposed to external risks. Consequently, patch density exhibits a negative correlation with the stability of regional landscapes. In a spatial cell, a lower diversity of LULC types, coupled with more complex shapes, results in the decreased stability of the cell, which, in turn, leads to an increase in the spatial conflict index [54]. The *SI* is calculated as follows:

$$PD = \frac{n_i}{A}, SI = 1 - PD \tag{5}$$

where n_i represents the number of patches of class i in the spatial unit; A refers to the area of the spatial unit; and PD refers to the denseness of the patches. An increase in the value of PD implies an increase in the degree of rupture of the one of the space, a decrease in its stability, and, at the same time, a corresponding decrease in its ability to withstand external disturbances.

In this paper, the grid tool of ArcGIS is employed to partition the study area into equal-sized grids, which serve as the fundamental units for evaluation. A comprehensive consideration of various influencing factors, including the extent of the study area and the characteristics of landscape patches, is undertaken. Following several comparisons, a spatial grid of 11 km $\times$ 11 km is selected for the division of the study area, resulting in a total of 1732 evaluation units. In this study, Fragstats was utilized to calculate the landscape ecological indicators for each spatial unit, and standardization of the results was performed during the calculation stage to ensure that the values ranged from 0 to 1 [55]. This standardization was necessary to derive the LUCI of the urban agglomeration. Building upon existing research findings [31,51–53] and the inverted U-shaped evolution law of spatial conflict, this paper employs the equidistant spacing method to categorize the levels of land use spatial conflict into four evaluation intervals (Table 1): mild conflict [0, 0.25), general conflict [0.25, 0.5), moderate conflict [0.5, 0.75), and severe conflict [0.75, 1].

Table 1. Indicators for determining the level of spatial conflict in land use.

Index	Level
$0.00 \leq$ LUCI < 0.25	Mild conflict
$0.25 \leq$ LUCI < 0.50	General conflict
$0.50 \leq$ LUCI < 0.75	Medium conflict
$0.75 \leq$ LUCI ≤ 1.00	Severe conflict

This study employs the global Moran's I index to evaluate the overall spatial correlation of land use conflicts. It analyzes the clustering and dispersal characteristics of the spatial conflict index and determines whether there is a general tendency towards spatial clustering or a more dispersed phenomenon. The values of the global Moran's I index range from −1 to 1. A value between 0 and 1 indicates a positive spatial autocorrelation, while a value between −1 and 0 signifies a negative spatial autocorrelation [56]. The formula is as follows:

$$I = \frac{n\sum_{i=1}^{n}\sum_{j=1}^{n} W_{ij}\left(S_i - \overline{S}\right)\left(S_j - \overline{S}\right)}{\sum_{i=1}^{n}\sum_{j=1}^{n}\left(S_i - \overline{S}\right)^2} \quad (6)$$

where I denotes the global Moran index, n represents the number of spatial units, S_i and S_j refer to the spatial conflict values at locations i and j, respectively, $\overline{S}$ is the average of the spatial conflict values in the study area, and W_{ij} represents a spatial weight matrix [56].

The global Moran's index has limitations when examining the local variation patterns of geographic elements. Spatial autocorrelation can differ due to local geographic variations [56]. Local autocorrelation is employed to investigate the phenomenon of local spatial clustering of conflicts, specifically to determine whether there are regions characterized by high or low levels of conflict. In this context, the local Moran's I index is introduced to quantify local spatial autocorrelation, which is calculated as follows:

$$LMI = \frac{\left(S_i - \overline{S}\right)}{M^2}\sum_{j=1}^{n} W_{ij}\left(S_j - \overline{S}\right) \quad (7)$$

where LMI represents the local Moran index, n represents the number of spatial cells, S_i and S_j refer to the spatial conflict values at i and j, respectively, $\overline{S}$ represents the average value of conflicts in the space where S_i is located, W_{ij} represents the spatial weight matrix, and M^2 represents the variance of the conflicts in the n spatial cells [56]. There are four categories of localized spatial features, and their degree of clustering and dispersion can be expressed as high–high (H–H), low–low (L–L), high–low (H–L), and low–high (L–H), respectively.

2.3.3. FLUS Model

The FLUS model is an innovative land use simulation model that predicts and demonstrates the future land use of the study area [57]. Its uniqueness lies in the introduction of spatial autocorrelation factors, including social, economic, and natural elements, through ANN. Additionally, it incorporates an adaptive inertia competition mechanism within the CA module, effectively addressing the instability associated with the inter-transformation of each class [58]. Furthermore, the FLUS model requires various parameters, such as neighborhood weights, target pixel inputs, and land use and cost matrices. Finally, Kappa and figure of merit (FoM) coefficients are employed as functions to assess the accuracy and feasibility of the model simulation.

The ANN mainly consists of input, hidden, and output layers [57] with the following expression:

$$p(p,k,t) = \sum_j W_{j,k}\ sigmoid\ \left(net_j(net_j(p,t))\right) = \sum_j W_{j,k} \times \frac{1}{1+e^{-net_j(p,t)}} \quad (8)$$

where $p(p,k,t)$ represents the probability of suitability of the k lands on grid p, time t; $W_{j,k}$ refers to the weights of the hidden layer and the output layer; *sigmoid* refers to the excitation function from the hidden layer to the output layer; and $net_j(p,t)$ refers to the signals received by the jth hidden layer grid p at time t [59].

The FLUS model simulates the dynamics of competition among various land types using an adaptive inertia mechanism that focuses on adjusting the adaptive inertia coefficients [59]. This coefficient is calculated based on the difference between the specific quantity of the current land type and the demand for land use. It self-adjusts during the iterative process with the objective of aligning the actual quantity of each land type with its intended target [60]. The expression governing this adjustment is as follows:

$$Interia_k^t = \begin{cases} Interia_k^{t-1}, \ if \left|D_k^{t-1}\right| \le \left|D_k^{t-2}\right|, \\ Interia_k^{t-1} \times \frac{D_k^{t-2}}{D_k^{t-1}}, \ if \ D_k^{t-1} < D_k^{t-2} < 0, \\ Interia_k^{t-1} \times \frac{D_k^{t-1}}{D_k^{t-2}}, \ if \ 0 < D_k^{t-2} < D_k^{t-1}, \end{cases} \tag{9}$$

where D_k^{t-1} and D_k^{t-2} are the difference between the raster data and the quantity demanded for the kth land at moments, where $t-1$ and $t-2$, respectively [61].

Based on the above approach, the likelihood of each raster change is measured, and classes are assigned to rasters everywhere using the iterative CA model [62]. The total probability $TP_{p,k}^t$, of a grid p being transformed into a site type k at moment t is expressed as follows:

$$TP_{p,k}^t = P_{p,k} \times \Omega_{p,k}^t \times Interia_k^t \times (1 - SC_{c \to k}) \tag{10}$$

where $SC_{c \to k}$ is the cost of converting land type c to k, $1 - SC_{c \to k}$ denotes the ease with which the conversion occurs, and $\Omega_{p,k}^t$ is the neighborhood role [61], which is formulated as follows:

$$\Omega_{p,k}^t = \frac{\sum_{N \times N} con\left(c_p^{t-1} = k\right)}{N \times N - 1} \times w_k \tag{11}$$

where $\sum_{N \times N} con\left(c_p^{t-1} = k\right)$ is the raster number of k classes of land after the end of iteration time $t-1$ on the $N \times N$ window, combined with the current land use status of the urban agglomeration on the north slope of Tianshan Mountain. This paper chooses to use a 3×3 Moore neighborhood model to calculate this parameter, and w_k is the weight of the role of each class of domain.

In land use demand forecasting, the fundamental aspect of the Markov model is to derive the transfer probability matrix of land types over the study period [63,64]. This matrix represents the probabilities of area or state transitions among various land use types, enabling accurate forecasts of land use states using the following formula:

$$S_{t+1} = P_{ij} \times S_t \tag{12}$$

where S_t, S_{t+1} is the land use state at the moment t, $t+1$; P_{ij} is the state transfer matrix [65].

The Kappa coefficient, introduced by Cohen in 1990, serves as a composite metric that integrates two key parameters: user accuracy and cartographic accuracy. Its primary purpose is to assess the accuracy of classified images [66]. The formula is as follows:

$$K = \frac{P_o - P_c}{1 - P_c} \tag{13}$$

where P_o is the proportion of correct simulation results, while P_c and 1 are the proportion of correct simulation results expected under random and ideal conditions, respectively [67]. The closer the Kappa value is to 1, the higher the simulation accuracy is, and when $0 < \text{Kappa} < 0.4$, it indicates that the consistency of the two graphs is low, that is, the simulation results are poor; when $0.4 < \text{Kappa} < 0.75$, it indicates that the consistency of the two graphs is general, that is, the simulation results are general; when the Kappa value is

greater than 0.75, it indicates that the simulation results are more consistent with the actual data, and the simulation results have higher credibility and feasibility [67].

The FoM index is considered a benchmark that indicates the consistency of the conversion patterns between real and simulated data. Its evaluation of land use change accuracy is superior to that of the Kappa coefficient [68]. The magnitude of this index is affected by the number of simulation years, with an increase of 1a per simulation year and an increase in the FoM index of no more than 0.01 as the standard level [69]. It is calculated using the following formula [70]:

$$FoM = \frac{B}{A + B + C + D} \tag{14}$$

where A represents the error caused by the fact that the land use changed in the real environment but the simulation stayed the same; B represents the fact that the real environment changed and at the same time the simulation correctly shifted accordingly; C represents the fact that the real environment changed and, at the same time, the simulation shifted, but the type of change did not correspond to the real situation, thus causing an error; and D represents the fact that the error caused by the fact that the real environment did not undergo a land use change, but the simulation shifted.

In this paper, ND, CP, and EP are identified as three distinct simulation scenarios. In the ND scenario, land use change from 1990 to 2020 is analyzed based on historical natural environmental conditions and human-driven factors, without accounting for policy planning constraints. The CP scenario incorporates findings from relevant research, whereby the probability of conversion from cultivated land to urban land is decreased by 60%, necessitating the strict implementation and enforcement of cultivated land protection policies [65,71]. In the EP scenario, the likelihood of forestland and grassland converting to urban land is reduced by 50%, while the probability of water bodies and cultivated land transitioning to urban land is diminished by 30%. Furthermore, the decrease in cultivated land is factored into the probability of conversion from cultivated land to forestland [65]. The FLUS model can be utilized to simulate LULC through various drivers, including natural, social, and economic factors [72]. These elements collectively influence the development of land landscapes, while geomorphology fundamentally shapes land use patterns. For instance, constructing cities in areas with steep slopes poses significant challenges, and high-altitude regions tend to exhibit lower population densities. Additionally, transportation and socioeconomic factors play a crucial role; proximity to railroads and highways facilitates transportation and accelerates urban development. Furthermore, population growth contributes to an abundant labor supply, thereby fostering economic advancement. Consequently, the natural drivers considered in this study encompass the digital elevation model (DEM), slope, slope direction, annual rainfall, average annual temperature, and the Normalized Difference Vegetation Index (NDVI). In contrast, the socioeconomic drivers include population density, GDP, and distances to railroads, roads, highways, rural areas, and towns (Figure 2).

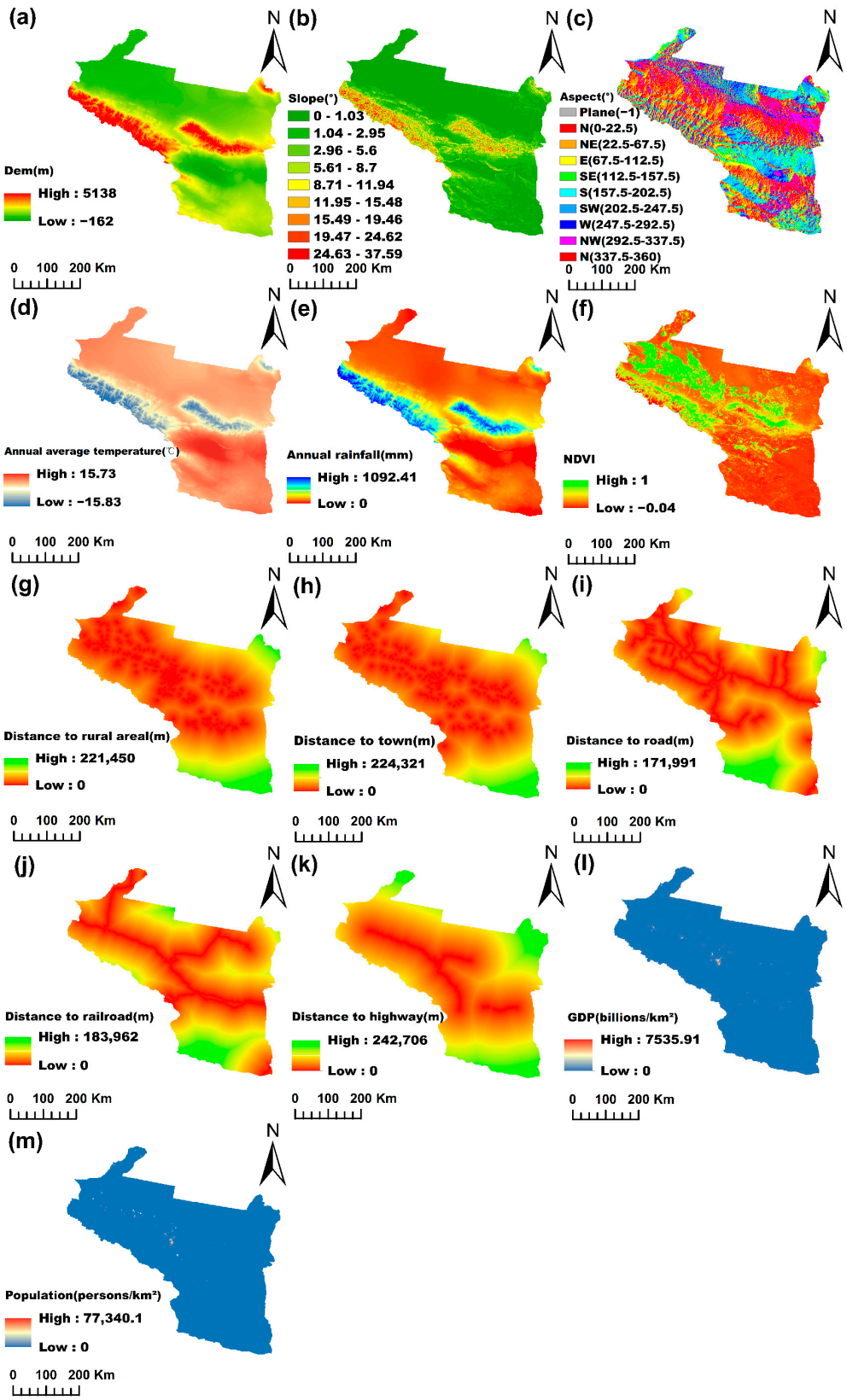

Figure 2. Drivers of land use, including DEM (**a**), slope (**b**), slope direction (**c**), average annual temperature (**d**), annual rainfall (**e**), NDVI (**f**), distance to rural areas (**g**), distance to towns (**h**), distance to roads (**i**), distance to railroads (**j**), distance to highways (**k**), GDP (**l**), and population (**m**).

3. Result

3.1. Analysis of LULC Changes

Figure 3 illustrates that farming, forestry, and grassland are widely distributed, forming a band that extends from west to east. Water bodies are concentrated in the Tianshan Mountain Range, located in the southwestern part of the study area, where elevations are higher. Influenced by topography, climate, and developmental context, urban land is primarily situated in the central region of the study area, exhibiting a tendency to expand westward. Because of the limitations set by the natural surroundings, substantial regions of unused land are present in both the northern and southern sections of the research area.

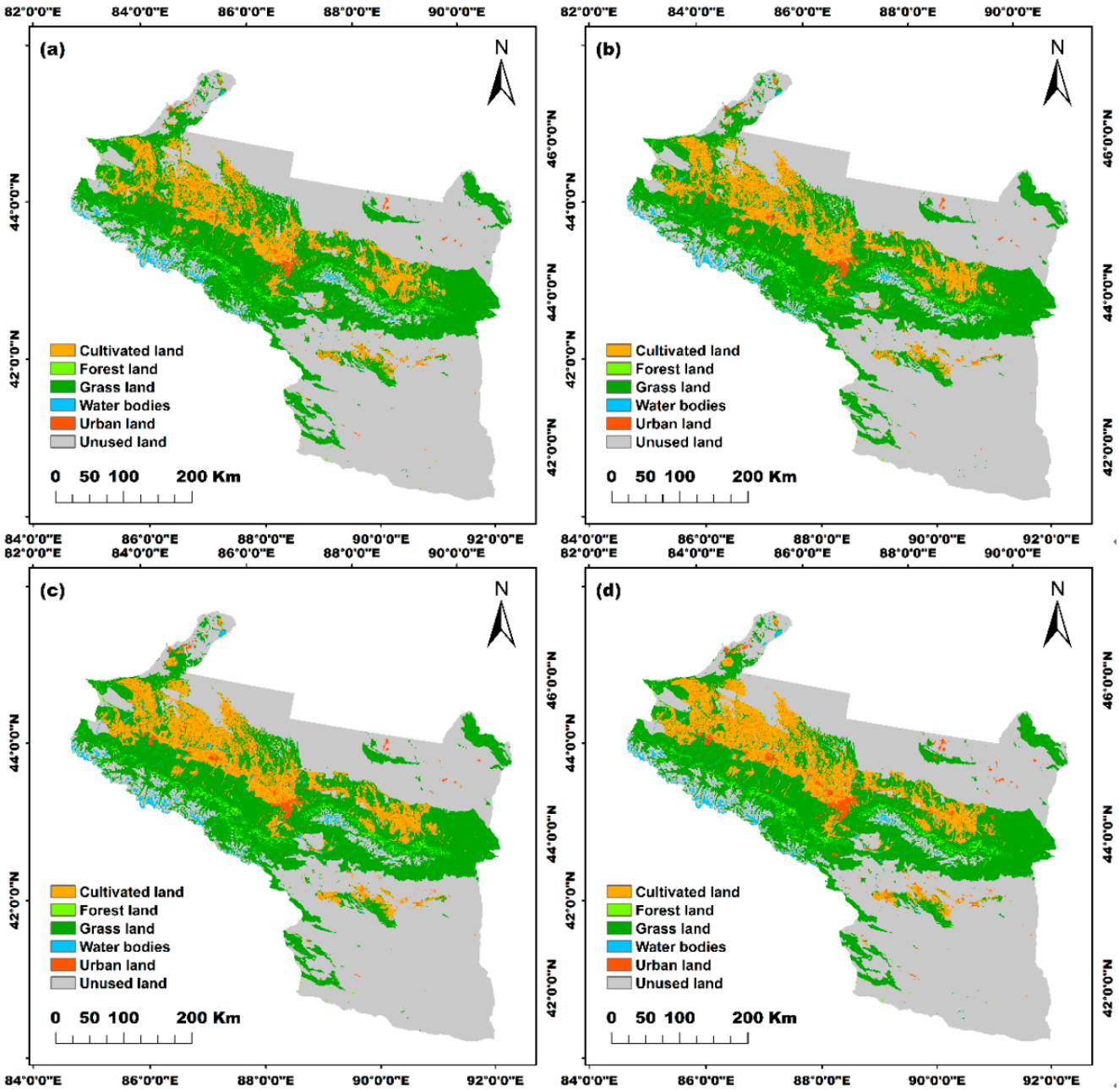

Figure 3. Spatial distribution of LULC in 1990 (**a**), 2000 (**b**), 2010 (**c**), and 2020 (**d**).

Table 2 demonstrates a continuous upward trend in the area of cultivated land throughout the study period, with an increase of 4960 km^2 compared to 1990, representing a change of 27.47%. Conversely, the area of forestland has consistently decreased by 354 km^2, reflecting a change of −10.26%. The grassland area also exhibited a downward trend during the study period, decreasing by 4347 km^2, or −7.15%, compared to the starting year of the study. In contrast, the total area of water bodies increased by 116 km^2, corresponding to a change of 7.12%. Throughout the study, the area of urban land displayed a rising trend, with an increase of 1457 km^2 from 1990 to 2020, amounting to a change of 77.55%, and the most significant increase occurred from 2010 to 2020, where it rose by 1088 km^2, reflecting a drastic change of 47.10%. Additionally, the area of unused land decreased by 1605 km^2, resulting in a change of −1.51%. In the urban agglomeration on the northern slopes of the Tianshan Mountains in Xinjiang, grassland and unused land are predominant. The land category with the largest area share is unused land, which accounted for over 50% in all years studied, while grassland comprised approximately 30% of the area. Cultivated land and urban land represented a small but increasing share over the study period, with water bodies accounting for the smallest share.

Table 2. Area (km^2)/share of each category (%) and magnitude of change (%) in different periods, 1990–2020.

Land Type	1990	1990–2000	2000	2000–2010	2010	2010–2020	2020	1990–2020
	Area/Area Proportion	Magnitude of Change	Area/Area Proportion	Magnitude of Change	Area/Area Proportion	Magnitude of Change	Area/Area Proportion	Magnitude of Change
Cultivated land	17,639/9.09	10.36	19,465/10.03	9.72	21,358/11.01	5.28	22,599/11.59	27.47
Forestland	2892/1.49	−8.93	2634/1.36	−1.27	2600/1.34	−0.19	2538/1.34	−10.26
Grassland	63,567/32.77	−2.31	62,096/32.01	−1.91	60,907/31.40	−3.09	59,220/30.43	−7.15
Water bodies	1635/0.84	6.01	1734/0.89	2.44	1776/0.92	−1.37	17,87/0.90	7.12
Urban land	1913/0.99	12.92	2160/1.11	6.89	2309/1.19	47.10	3370/1.75	77.55
Unused land	106,345/54.82	−0.42	105,902/54.59	−0.81	105,040/54.15	−0.29	104,779/53.99	−1.51

From 1990 to 2020, the areas of cultivated land, water bodies, and urban land in the urban agglomeration of the northern slope of the Tianshan Mountain in Xinjiang exhibited an increasing trend. Conversely, the areas of forestland, grassland, and unused land demonstrated a decreasing trend, with urban land experiencing the most significant growth. This urban expansion is closely linked to rapid socioeconomic development, an accelerated urbanization process in recent years, and relevant policies implemented in the study area. As urban development progressed, living conditions, infrastructure, and healthcare services improved, leading to an increase in the urban population and heightened pressure on food resources. As a result, the amount of land used for agriculture increased, and improvements in water management infrastructure played a significant role in the enlargement of water bodies within the area. In response to the needs of production and habitation, forested areas, grasslands, and idle lands have been transformed into agricultural and urban spaces, leading to a decrease in their respective sizes.

3.2. LULC Prediction Under Different Scenarios

The Kappa coefficient and the FoM index were employed to validate the results of the land use prediction. The calculated Kappa coefficients for the ND, CP, and EP scenarios were 0.94736, 0.952826, and 0.9654, respectively, while the corresponding FoM coefficients were 0.0891815, 0.0598824, and 0.0493119, respectively. These results indicate a high level of accuracy in the simulation, providing a reliable basis for forecasting future land use changes. This model and its related parameters can be further analyzed for land use prediction, as illustrated in Figure 4 and Tables 3–5.

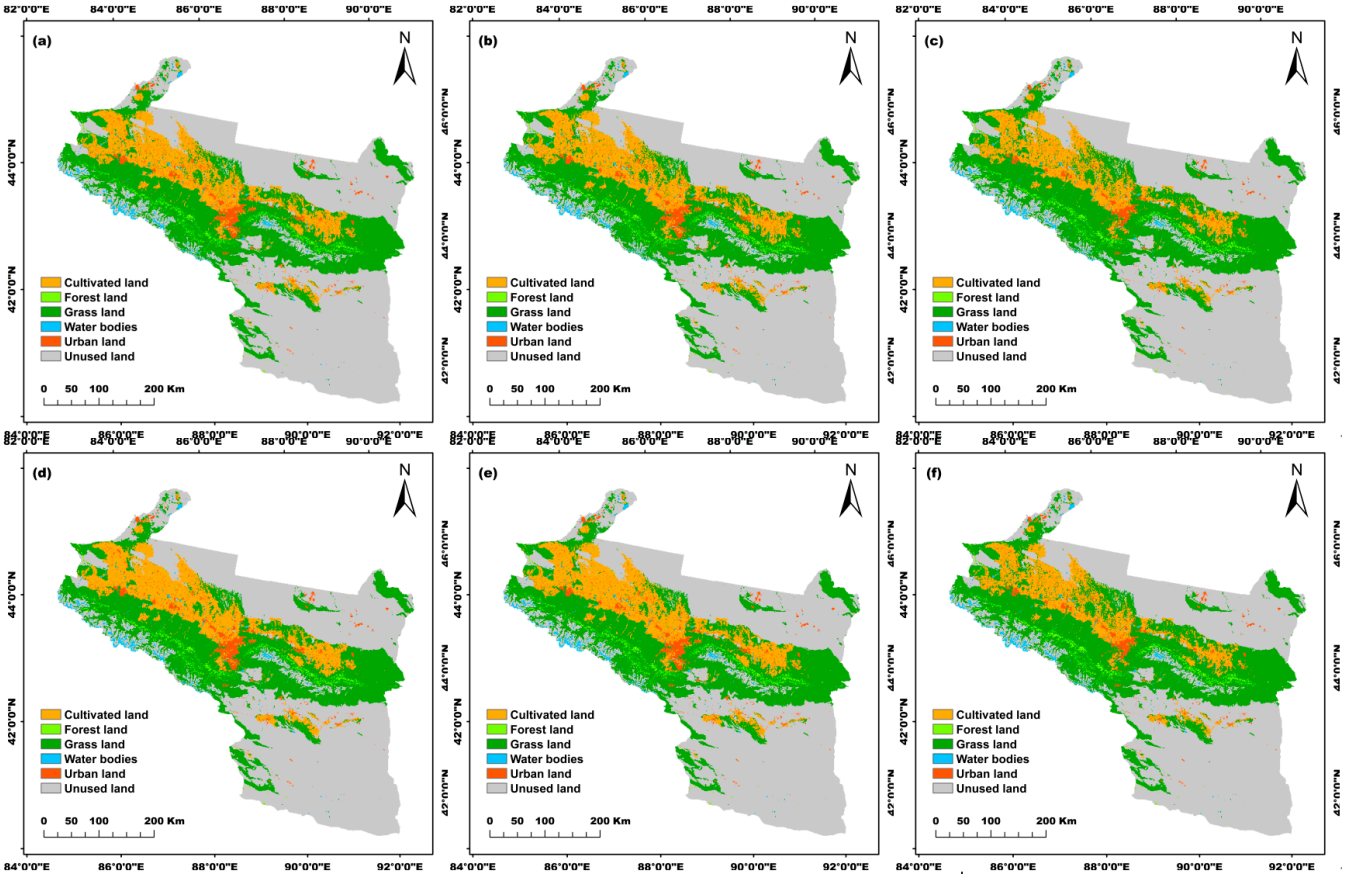

Figure 4. Spatial distribution of predicted LULC in 2030 under ND (**a**), CP (**b**), and EP (**c**), and in 2050 under ND (**d**), CP (**e**), and EP (**f**).

Table 3. Area of each land use type in 2030 and 2050 under the ND scenario (km^2).

Year	Cultivated Land	Forestland	Grassland	Water Bodies	Urban Land	Unused Land
2020	22,599	2538	59,220	1787	3370	104,779
2030	23,611	2536	57,588	1772	4313	104,473
2050	25,393	2532	56,246	1743	4504	103,875

Table 4. Area of each land use type in 2030 and 2050 under the CP scenario (km^2).

Year	Cultivated Land	Forestland	Grassland	Water Bodies	Urban Land	Unused Land
2020	22,599	2538	59,220	1787	3370	104,779
2030	23,668	2536	57,610	1772	4234	104,473
2050	25,714	2532	56,264	1743	4186	103,854

Table 5. Area of each land use type in 2030 and 2050 under the EP scenario (km^2).

Year	Cultivated Land	Forestland	Grassland	Water Bodies	Urban Land	Unused Land
2020	22,599	2538	59,220	1787	3370	104,779
2030	20,599	2649	61,325	1809	3435	104,476
2050	19,740	2759	62,643	1822	3458	103,871

Under the ND scenario, the areas of cultivated and urban land are projected to increase significantly by 2030 and 2050, with increases of 2794 km^2 and 1134 km^2 over the next 30 years, respectively. In contrast, the areas of the remaining land categories are expected to experience a decline. The growth in cultivated and urban land is primarily concentrated in the central and western regions of the study area, largely resulting from encroachment on grassland, with a smaller contribution from unused land. Meanwhile, forested land and grassland are anticipated to show only a modest decline, and, overall, there are expected to be no significant changes.

Under the CP scenario, the changes in the spatial patterns of land use projected for 2030 and 2050 closely resemble those of the ND scenario. Specifically, both cultivated land and urban land are expected to increase significantly, with cultivated land expanding by 3115 km^2 and urban land by 816 km^2 over the 30-year period. However, in comparison to the ND scenario, the area of cultivated land exhibits a more pronounced increase in both 2030 and 2050, while the growth rate of urban land area appears to decelerate. This deceleration is primarily attributed to the conversion of larger tracts of grassland into cultivated land and certain restrictions on urban expansion, which collectively enhance the security of cultivated land holdings. Meanwhile, the changes in forestland and water bodies are projected to remain relatively minor.

Under the EP scenario, the land categories projected to increase in area include forestland, grassland, water bodies, and urban land, with respective increases of 221 km^2, 3423 km^2, 35 km^2, and 88 km^2 over the next 30 years. In contrast, the areas of cultivated land and unused land are expected to decrease significantly, with reductions of 2859 km^2 and 908 km^2, respectively. This scenario operates by restricting the conversion of forestland and grassland, thereby promoting the harmonious development of both the economy and ecology. Simultaneously, while ensuring that the basic arable land remains unchanged, portions of the cultivated land will be transitioned to forests and grassland, and parts of the existing forest and grassland will undergo restoration and conservation efforts. These measures are intended to enhance the stability of forest and grassland ecosystems and increase their respective areas, particularly in the central and western regions of the study area, where forest, grassland, and cultivated land are intermingled. Urban expansion has been notably curtailed due to ecological protection measures, resulting in a deceleration of urban land growth. Consequently, the increase in forest and grassland areas, along with the slowed urban development, has contributed to the further protection of water bodies, resulting in a modest increase in their area.

3.3. Land Use Spatial Conflict Measurement and Analysis

3.3.1. LUCI Analysis

The normalization and visualization of the LUCI revealed the spatial distribution of land use conflicts in the study area from 1990 to 2020 (Figure 5). Throughout this period, the LUCI for the urban agglomeration on the northern slopes of the Tianshan Mountains predominantly fell within the general conflict zone, particularly in the northern and southern regions of the study area. These regions encompass extensive areas of unused land, as well as vast deserts, gobi, and mountain ranges characterized by extremely harsh environments, resulting in a sparsely populated landscape. Consequently, land use in these areas is less susceptible to human disturbances, leading to relatively low spatial conflicts. Additionally, forestland is predominantly situated in this region and is influenced by ecological protection policies that help maintain low levels of spatial conflict. Very few areas are in the heavy conflict interval, as this is primarily in the water bodies in the central and southwestern portions of the study area. The LUCI in parts of the western and central regions is in the medium conflict zone, and these regions are mainly at the junction of

cultivated land, cultivated forest and grassland, and unused land at high altitude, which is mainly related to the regional land use demand, and with the accelerated process of urbanization. As the population of the study area increases, the demand for cultivated land increases, and human beings cut down a large amount of forest and grassland and turn it into arable land, leading to intense spatial land use conflicts in the region. Furthermore, the high-altitude unused land in the west is covered by extensive snow year-round, and the formation and melting of snow and ice, influenced by temperature fluctuations, result in frequent changes to its landscape pattern. The area in mild conflict is in the shape of a band running through the east and west ends of the study area, and the main land use type in this area is grassland; under the implementation of the government's ecological protection policy, the spatial conflict level in this area shows a low level.

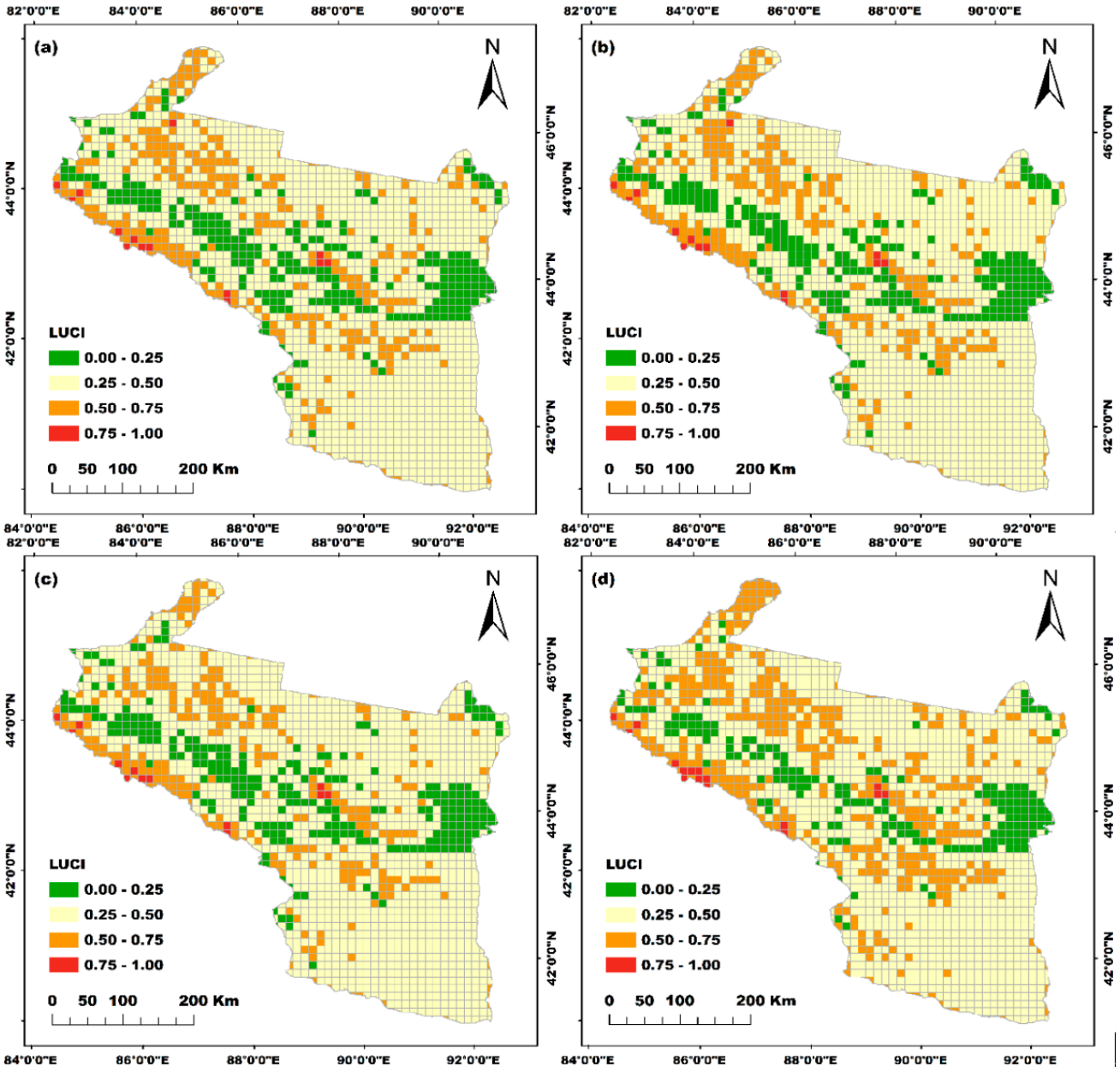

Figure 5. Spatial distribution of the LUCI in 1990 (**a**), 2000 (**b**), 2010 (**c**), and 2020 (**d**).

Table 6 illustrates that the LUCI exhibits both a downward and subsequent upward trend, ultimately revealing an overall upward trajectory. The LUCI is predominantly influenced by general conflicts, while the percentage of units in the region shows a fluctuating trend, increasing from 63.28% in 1990 to 65.47% in 2010, before declining to 60.33% in 2020. This is followed by medium conflict, where the share of units in this category significantly rises over the 30-year period, from 20.32% in 1990 to 27.25% in 2020. Conversely, the number of mildly conflicted units has decreased markedly throughout the study period. Although the share of severe conflict has remained the smallest, it has seen a slight increase alongside urban expansion and population growth, rising by 0.23% from 1990 to 2020. These findings indicate that during the study period, land use conflicts in the urban agglomeration on the north slope of Tianshan Mountain were not intense, suggesting a reasonable utilization of land resources and stable, coordinated land use development. However, with the acceleration of the urbanization process, there are indications that land conflicts are beginning to intensify.

Table 6. Changes in the time series of the LUCI between 1990 and 2020.

LUCI Interval	Index	Number of Space Units/Cell				Percentage of Space Units/%			
		1990	2000	2010	2020	1990	2000	2010	2020
Mild conflict	0.00–0.25	263	256	261	190	15.18	14.78	15.07	10.97
General conflict	0.25–0.50	1096	1110	1134	1045	63.28	64.09	65.47	60.33
Medium conflict	0.50–0.75	352	345	317	472	20.32	19.92	18.30	27.25
Severe conflict	0.75–1.00	21	21	20	25	1.21	1.21	1.15	1.44
Aggregate		1732	1732	1732	1732	100	100	100	100
Average value		0.41	0.40	0.40	0.44				

3.3.2. Characterization of Spatial Differentiation in Spatial Land Use Conflicts

In the global spatial autocorrelation analysis, the global autocorrelation coefficient, known as Moran's I, was calculated for the study area, and its significance was assessed using the *p*-value (Figure 6 and Table 7). The values of Moran's I for the urban agglomeration on the north slope of Tianshan Mountain in 1990, 2000, 2010, and 2020 were 0.528, 0.522, 0.517, and 0.511, respectively, all of which were positive. A larger absolute value of Moran's I indicates a higher degree of positive autocorrelation in the spatial conflict of land use. The *p*-values for all periods were less than 0.01, suggesting that the LUCI exhibits positive spatial autocorrelation and tends to cluster spatially with a confidence level of 99%. Furthermore, upon examining the distribution of the LUCI, it was observed that most of the conflict scatter was concentrated in quadrants 1 and 3, characterized by high-high H-H and L-L aggregation patterns. In terms of temporal trends, Moran's I demonstrates a decreasing pattern, with values declining from 0.528 in 1990 to 0.511 in 2020, while still maintaining a high level of significance. This trend indicates a reduction in the spatial aggregation of the LUCI in the study area, suggesting that the correlation among various conflicts is weakening. The Z-values for the four periods were 42.1617, 41.9209, 42.1659, and 42.3451, respectively. A larger Z-value signifies a more significant correlation, indicating that the test results are highly significant.

Table 7. Global Moran's I of the LUCI.

Year	Moran's I	Z	*p*
1990	0.528	42.1617	0.001
2000	0.522	41.9209	0.001
2010	0.517	42.1659	0.001
2020	0.511	42.3451	0.001

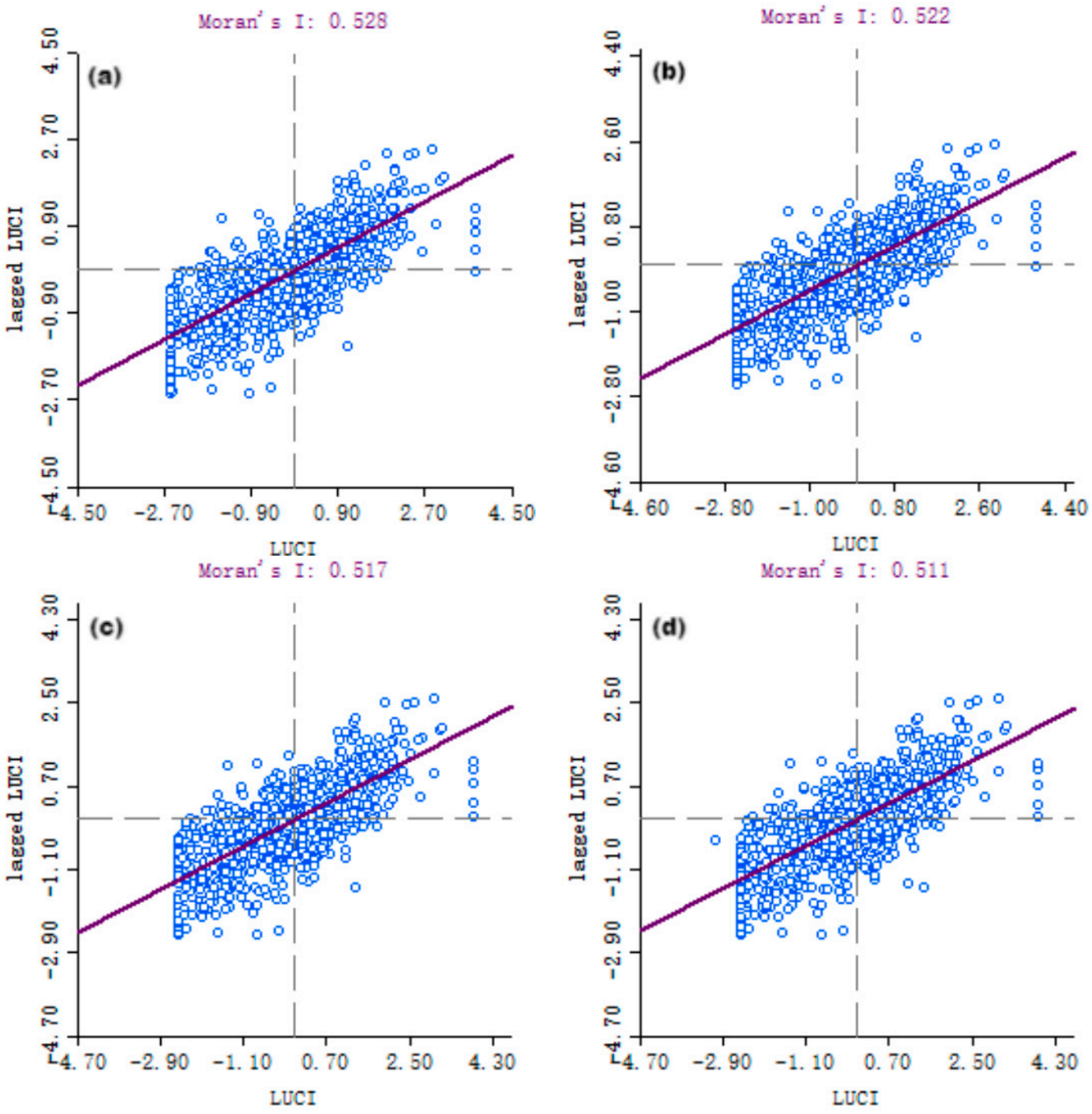

Figure 6. Moran scatterplot of the LUCI in 1990 (**a**), 2000 (**b**), 2010 (**c**), and 2020 (**d**).

Figures 7 and 8 illustrate that the *p*-values derived from the four-period data of the urban agglomeration on the north slope of Tianshan Mountain, spanning from 1990 to 2020, are all below 0.05. This indicates that they pass the 95% confidence test, signifying significant local spatial autocorrelation of the LUCI for each spatial unit. Notably, land use conflicts exhibit distinct spatial distribution patterns. The areas of H-H aggregation are primarily located in the central and northwestern parts of the study region, which include urban areas as well as agricultural and pastoral lands. These regions may experience heightened disturbances from human activities, resulting in less stable land use systems and more complex landscape units. Consequently, areas with elevated levels of conflict tend to cluster together in these regions. Additionally, climate warming has contributed to glacier melting and alterations in the landscape patterns of high-altitude areas in the southwest, which also display a notable trend of high-value aggregation. Conversely, L-L

agglomerations are primarily found in the grassland zones of the study area, characterized by larger sizes and a relatively minor degree of human modification. Due to the stable natural ecology and certain protective policies in place, the landscapes in these areas remain less damaged, and landscape connectivity is stronger, leading to the clustering of regions with low conflict levels.

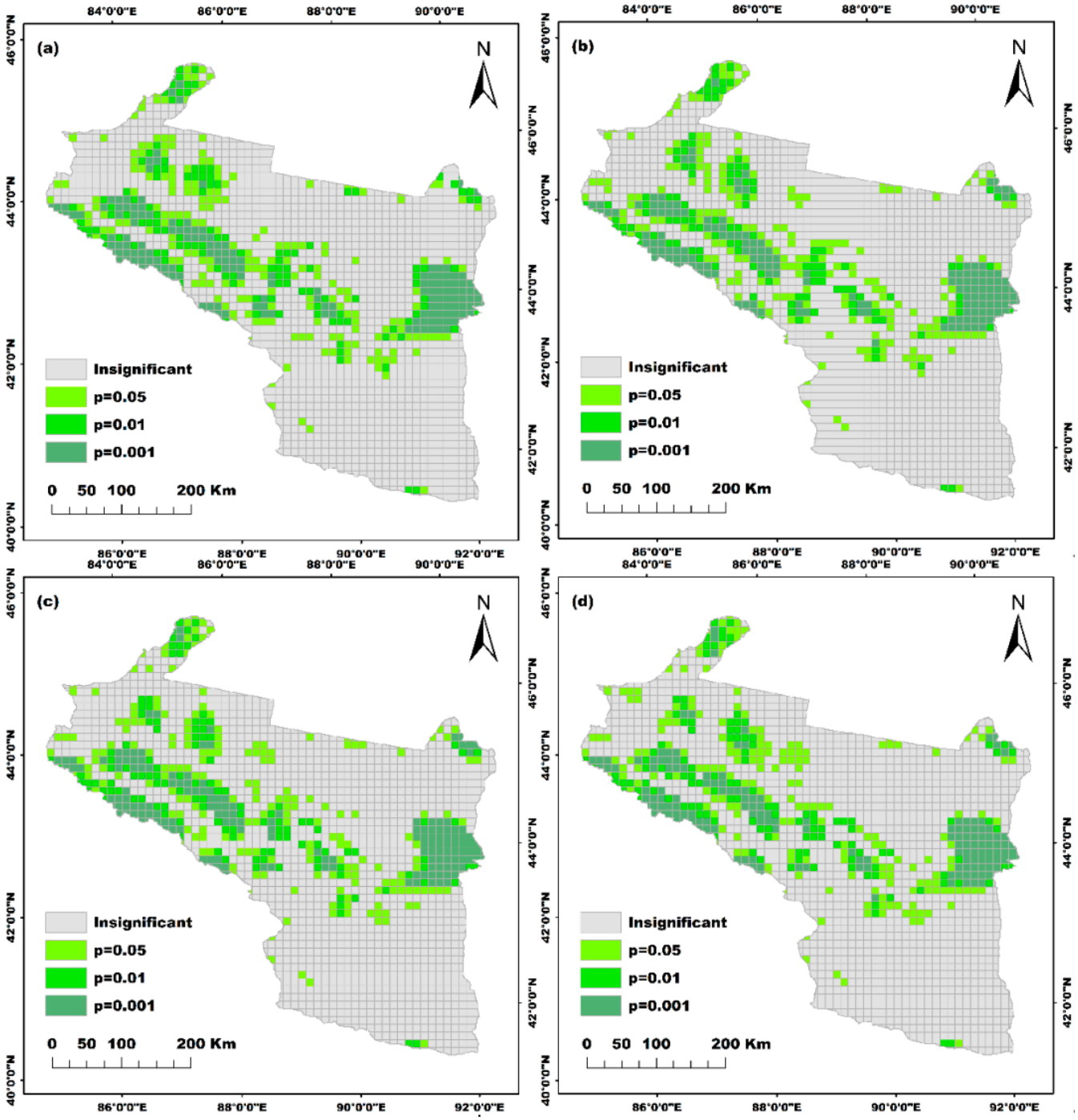

Figure 7. Localized significance maps of spatial land use conflicts in 1990 (**a**), 2000 (**b**), 2010 (**c**), and 2020 (**d**).

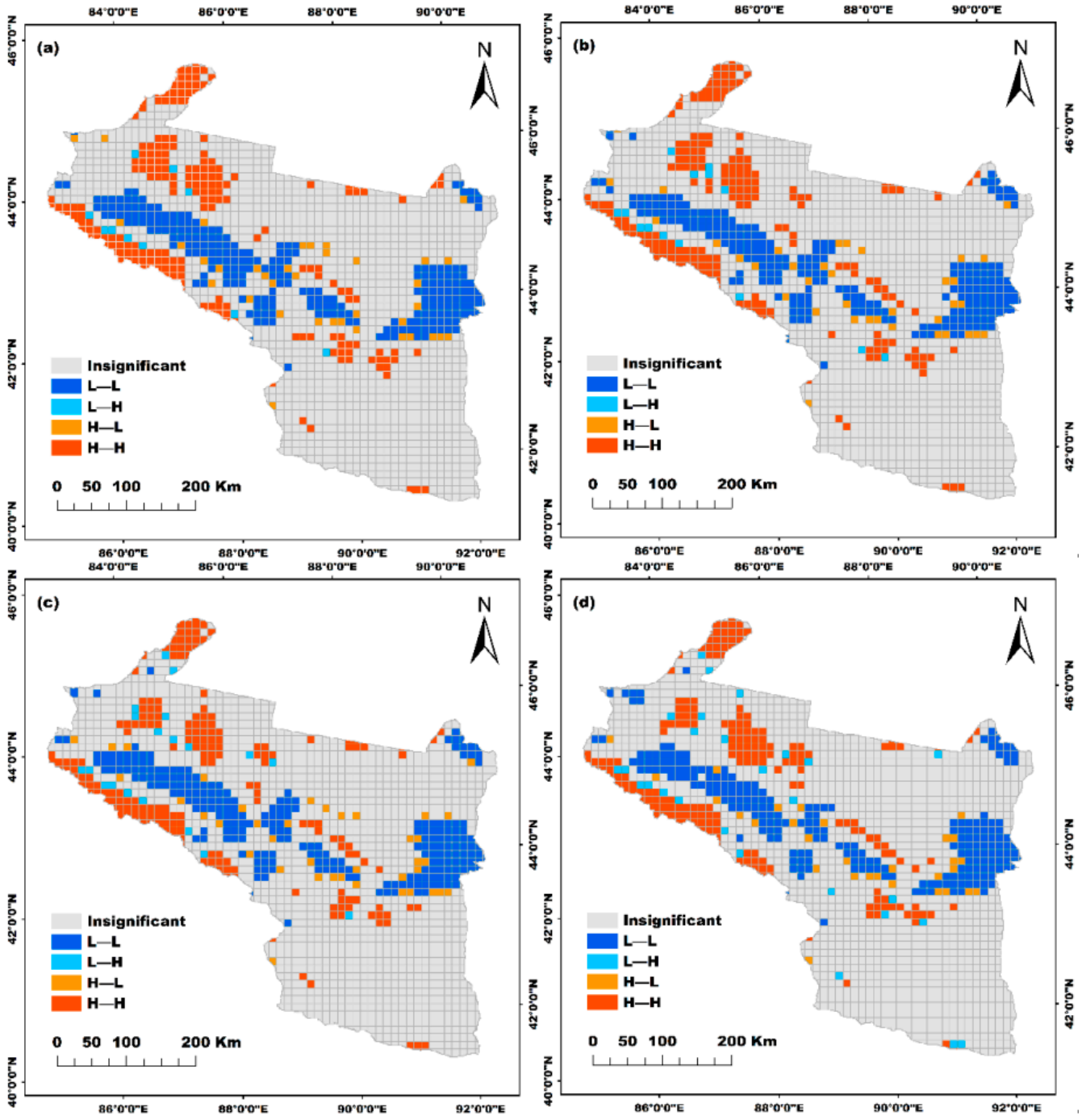

Figure 8. Local autocorrelation Lisa clustering of spatial land use conflicts in 1990 (**a**), 2000 (**b**), 2010 (**c**), and 2020 (**d**).

3.3.3. Simulation of the LUCI in Different Future Scenarios

A landscape pattern perspective was employed to further examine and analyze the spatial distribution and temporal sequence of future land use spatial conflicts (Figure 9 and Tables 8–10). Under the ND scenario, the mean value of the LUCI in the urban agglomeration on the northern slope of Tianshan Mountain is projected to increase by 0.02 from 2020 to 2050, indicating a trend of gradual escalation. In both 2030 and 2050, LUCI is predominantly characterized by general conflict, comprising 61.20% and 59.24% of the total, respectively, which reflects an overall decreasing trend. This is followed by medium conflict, which accounts for 26.62% and 31.29%, respectively, demonstrating an overall upward trend. Conversely, mild and severe conflicts exhibit decreasing and increasing

trends, respectively. Medium conflict experiences the most significant change, with an increase of 4.04%, while mild conflict shows a decrease of 3.41%. The scenario indicates a transformation of mild and general conflicts into moderate and severe conflicts within the study area from 2020 to 2050, suggesting a tendency for spatial land use conflicts to intensify.

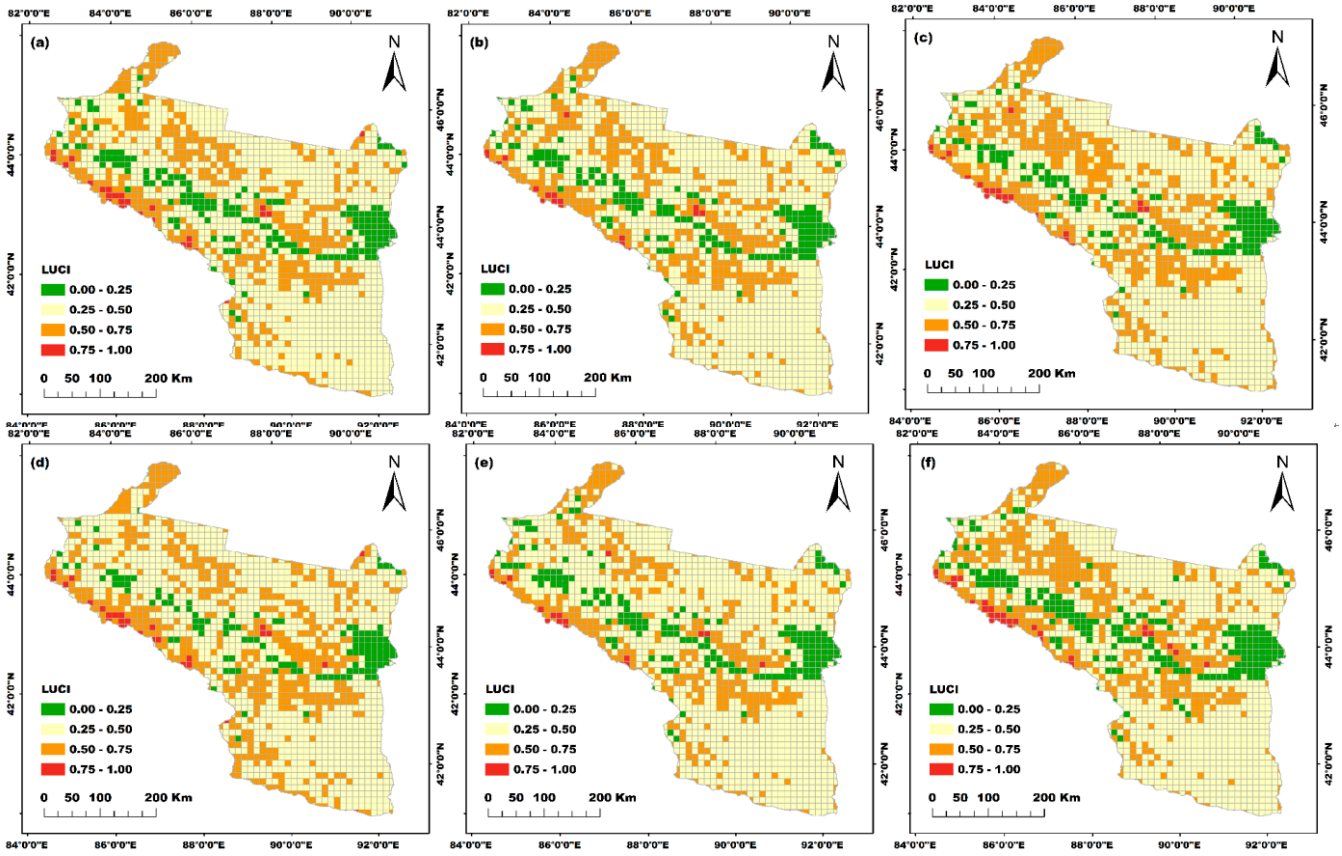

Figure 9. Spatial distribution of predicted LUCI in 2030 under ND (**a**), CP (**b**), and EP (**c**), and in 2050 under ND (**d**), CP (**e**), and EP (**f**).

Table 8. Time-series changes in LUCI in 2030 and 2050 under the ND scenario.

LUCI Interval	Index Band	Number of Space Units/Cell			Percentage of Space Units/%		
		2020	2030	2050	2020	2030	2050
Mild conflict	0.00–0.25	190	180	131	10.97	10.39	7.56
General conflict	0.25–0.50	1045	1060	1026	60.33	61.20	59.24
Medium conflict	0.50–0.75	472	461	542	27.25	26.62	31.29
Severe conflict	0.75–1.00	25	31	33	1.44	1.79	1.91
Aggregate		1732	1732	1732	100	100	100
Average value		0.44	0.45	0.47			

Table 9. Time-series changes in LUCI in 2030 and 2050 under the CP scenario.

LUCI Interval	Index Band	Number of Space Units/Cell			Percentage of Space Units/%		
		2020	2030	2050	2020	2030	2050
Mild conflict	0.00–0.25	190	175	179	10.97	10.10	10.33
General conflict	0.25–0.50	1045	1046	1086	60.33	60.39	62.70
Medium conflict	0.50–0.75	472	484	440	27.25	27.94	25.40
Severe conflict	0.75–1.00	25	27	27	1.44	1.56	1.56
Aggregate		1732	1732	1732	100	100	100
Average value		0.44	0.45	0.44			

Table 10. Time-series changes in LUCI in 2030 and 2050 under the EP scenario.

LUCI Interval	Index Band	Number of Space Units/Cell			Percentage of Space Units/%		
		2020	2030	2050	2020	2030	2050
Mild conflict	0.00–0.25	190	154	210	10.97	8.89	12.12
General conflict	0.25–0.50	1045	996	975	60.33	57.51	56.29
Medium conflict	0.50–0.75	472	549	507	27.25	31.70	29.27
Severe conflict	0.75–1.00	25	33	40	1.44	1.91	2.31
Aggregate		1732	1732	1732	100	100	100
Average value		0.44	0.46	0.44			

Under the CP scenario, the LUCI in the study area exhibits an initial increase followed by a decrease from 2020 to 2050, resulting in no significant overall change. Land use conflicts in 2030 and 2050 are primarily characterized by general conflicts, which account for 60.39% and 62.70% of conflicts in these years, respectively, indicating an upward trend. This is followed by medium conflicts, which comprise 27.94% and 25.40%, respectively, demonstrating a declining trend. The proportion of mild conflicts remains stable at approximately 10%, although their area decreases over the next 30 years. The incidence of severe conflicts is minimal and shows no significant change. From 2020 to 2050, the most notable change occurs in general conflicts, which increase by 2.37%, while medium conflicts decrease by 1.85%, mild conflicts decrease by 0.64%, and severe conflicts show a slight increase of only 0.12%, remaining unchanged from 2030 to 2050. In summary, the level of land use spatial conflicts in the study area under the CP scenario remains well-regulated, with certain areas experiencing a transition from medium conflicts to general conflicts. This scenario appears to effectively promote the coordinated development of spatial land use conflicts within the region.

Under the EP scenario, the LUCI exhibits an initial increase followed by a decrease from 2020 to 2050, with its mean value returning to 0.44 in 2050, consistent with the value in 2020. The study areas for 2030 and 2050 are predominantly characterized by general conflict, accounting for 57.51% and 56.29%, respectively, reflecting an overall decreasing trend. This is followed by medium conflict, which comprises 31.70% and 29.27%, respectively, indicating an upward trend. Both mild and severe conflicts are projected to rise over the next 30 years, peaking in 2050. Notably, mild conflicts exhibit the most significant change, with a 4.04% reduction in their share, whereas medium conflicts see an increase of 2.02%. Over the next 30 years, mild and severe conflicts are expected to rise by 1.15% and 0.87% in their spatial unit share, respectively. There is a notable increase of 3.23% in the share of mild conflicts from 2030 to 2050, while medium conflicts display a significant downward trend during this period, with a decreasing ratio of 2.43. Meanwhile, the decline in the share of general conflicts has slowed. In summary, under the EP scenario, the level of land use spatial conflicts in the study area is maintained at a satisfactory level from 2020 to 2050. Although there is an overall decrease in general conflicts and an increase in medium conflicts, these trends are moderated or even reversed between 2030 and 2050, suggesting that the scenario positively influences the future regulation of land use spatial conflicts in the study area.

4. Discussion

4.1. Identification of Land Use Spatial Conflicts

4.1.1. Methods for Identifying Spatial Conflicts in Land Use

Land use and development activities are primarily determined at the landscape level, meaning that all economic activities related to land occur within the spatial context of the landscape [73]. According to landscape ecology principles, different land use methods and intensities produce distinct ecological effects, which can be directly observed in the land-

scape pattern, subsequently leading to alterations in the terrestrial landscape. Moreover, changes in landscape patterns can significantly influence ecological processes [74]. Both human actions and natural factors contribute to modifications in the spatial configuration of the landscape, thereby affecting the level of conflict. In this study, we established an assessment model of the LUCI based on landscape patterns. From 1990 to 2020, the conflict level exhibited a trend of initially weakening and then increasing. Overall, the average LUCI value rose by 0.03, with the most pronounced increases occurring in built-up areas, cultivated land, and other regions characterized by frequent human activities. This trend indicates a gradual deterioration, aligning with findings from existing research [75,76]. The proposed spatial conflict measurement method is deemed appropriate for analyzing the LUCI and its distribution pattern.

4.1.2. Analysis of the Relationship Between Spatial Land Use Conflicts and Land Use

The evolution of spatial land use conflicts serves as a comprehensive reflection of regional development and its spatial microcosm in land use [77]. Various development activities generate contradictions and conflicts in the utilization of land resources, leading to spatial conflicts in land use that adversely affect the socioeconomic and ecological environment [29]. Research indicates that large areas of unutilized land, such as deserts, mountains, and hills, are distributed within the urban agglomerations on the northern slopes of Tianshan Mountain. This results in land use conflicts primarily characterized by general conflicts. In the study conducted by Tian et al., it was noted that Urumqi is surrounded by mountains on three sides, exhibiting a lack of conflicts and a prevalence of mild conflicts, which aligns with the findings of this paper [78]. Land use spatial conflict levels are higher in areas characterized by significant human activity, such as cultivated and urban lands, compared to lower levels of conflict observed in forestland, grassland, and water bodies. Between 2010 and 2020, the percentage of cultivated land in the study area increased by 0.58%, while urban land area rose by 0.56%, marking the most substantial changes during this period. The mean value of the LUCI experienced the most pronounced increase, rising from 0.40 to 0.44. This trend indicates that the expansion of built-up areas and cultivated land, driven by population growth during this time, has rendered the landscape pattern of the region increasingly fragmented. Consequently, the conflict between people and land has significantly intensified, corroborating the findings of the study conducted by Lv et al. [29]. Additionally, research by Chen Zhu'an et al. demonstrated that the substantial growth of urban and cultivated areas further exacerbated land fragmentation in Nanchang City, with the average land conflict level escalating from 0.19 to 0.33 between 1995 and 2015 [52]. Furthermore, Niu et al. investigated spatial land use conflict in the "three life" space of Jinan City, revealing that the average water conflict value increased from 0.49 to 0.56 from 2010 to 2020 [79]. From 2000 to 2010, the vigorous implementation of ecological protection measures successfully maintained the areas of forest and grassland, resulting in a 0.39% increase in the proportion of grassland during this period. Additionally, the mean value of the LUCI remained stable, indicating a reduction in human–land conflicts. This suggests that limiting the expansion of built-up areas and cultivated land into forest and grassland positively contributes to maintaining landscape connectivity and mitigating land conflicts. Chen et al. demonstrated that the forest coverage rate in Guiyang City increased from 14.5% to 55% between 1990 and 2020, while the green space rate in built-up areas rose by 10.2%. Consequently, the urban ecological carrying capacity was enhanced, and land use conflicts were diminished [75], aligning with the findings of this study.

In the various scenarios simulated for the years 2020 to 2050, the mean value of the LUCI increases from 0.44 to 0.47 in the ND scenario, while it remains constant at

0.44 in the other two scenarios. Observations of landscape patterns reveal that, in the ND scenario, the absence of government and planning restrictions leads to heightened land use conflicts, significant exploitation of forest and grassland, and severe ecological degradation. In the CP scenario, cultivated land encroaches more extensively on large areas of grassland, leading to increased land use conflicts. Conversely, in the EP scenario, forest and grassland are effectively protected; however, urban development faces constraints, which may hinder economic growth and raise potential food security concerns due to the considerable reduction in cultivated land area. The varying scenario settings exert different degrees of influence on the future changes across each category. Consequently, a single scenario is insufficient to optimize the spatial pattern of land use in the study area adequately. Therefore, it is essential to consider multi-scenario co-development, integrating diverse policies and plans based on clearly defined development needs and objectives, to facilitate a more rational allocation of land use, optimize spatial patterns, and achieve harmonious development between humanity and nature.

4.2. Policies and Recommendations

First, it is essential to clearly delineate development boundaries in the urban core area to effectively manage the disorderly expansion of the city, ensuring that urban development occurs within the established planning framework and minimizing resource waste and environmental damage. Second, it is crucial to promote the upgrading of the industrial structure, reducing overreliance on land resources and enhancing land use efficiency by adjusting and optimizing the industrial framework. In regions characterized by high-quality cultivated land, including permanent basic farmland and major agricultural production zones, a stringent land protection model will be enforced. This approach aims to prevent the degradation of high-quality cultivated areas and to safeguard food security. Furthermore, the urban agglomeration on the northern slopes of the Tianshan Mountains is home to a significant number of farmers and herdsmen, who depend on arable land for their livelihood through agricultural production. Consequently, it is vital to promote socioeconomic development while preserving ecological integrity, to create more employment opportunities for farmers and herders, and to transition the economic development model in certain areas, thereby limiting the expansion of arable land in the near future. The optimization of traffic roads is one method to alleviate land use conflicts. In planning urban transportation, it is essential to minimize the routing of roads and railways through the core areas of the reserve. Additionally, restoration activities should be implemented in forested and grassland areas.

4.3. Limitations and Prospects

This study proposes a comprehensive index model for measuring spatial conflict in land use, with a particular emphasis on the complexity, vulnerability, stability, and dynamic changes inherent in land use systems. The model is intended to provide a comprehensive assessment of the spatial conflict arising from land use. In fact, land use conflict encompasses a multitude of dimensions, including but not limited to the following: land use system conflict, land use social conflict, and land use ecological mitigation conflict. These diverse facets necessitate a comprehensive research agenda for posterity. Future research should integrate multiple evaluation methods, adopt diverse perspectives, and combine qualitative and quantitative assessments to more comprehensively measure and evaluate land use conflicts, thereby constructing a more robust research framework. Furthermore, when simulating the spatial patterns of land use over extended time frames, the results of this study may exhibit inaccuracies due to the elasticity effect of the FLUS model. Future investigations should consider selecting a more appropriate and precise predictive model

to enhance the accuracy and reliability of the results, thereby improving the scientific rigor of the study. Additionally, during the identification of driving factors, only those that can be quantified were included, given the inherent characteristics of the FLUS model and the accessibility of data. However, certain factors, such as policy and natural influences, are challenging to quantify in the context of land use evolution. Therefore, it is imperative to address how to incorporate these influences into the model in future research.

5. Conclusions

This research evaluates the intensity of spatial conflicts related to land use by utilizing a landscape pattern viewpoint to assess alterations in conflict intensity across time and space throughout the duration of the study. Finally, the FLUS software (FLUS_V2.4) is utilized to simulate the spatial pattern of land use in the urban agglomeration for the years 2030 and 2050 under three scenarios: ND, CP, and EP. Based on these simulations, the study predicts the spatial conflicts of land use in the area under different scenarios. The results indicate the following:

(1) Land use has changed significantly from 1990 to 2020. In terms of land use types, unused land is the most dominant category in the study area, primarily due to the extensive presence of desert and gobi regions, which are characterized by harsh natural conditions that hinder both natural evolution and human transformation. Additionally, grassland is the most widely distributed land type in the area. Regarding changes in land types, there is an increasing trend in the areas of cultivated land, water bodies, and urban land, while the areas of forestland, grassland, and unused land are decreasing. The accelerated urbanization process has particularly highlighted the increase in urban land, while the encroachment of cultivated and urban land on grassland has resulted in a notable reduction in grassland area.

(2) The spatial and temporal changes in land use conflicts within the study area are evident. The classification of conflicts for each year is as follows: general conflict > medium conflict > mild conflict > severe conflict. Notably, the proportion of general conflicts has consistently remained above 60% across all periods, indicating its dominance. From 1990 to 2020, the LUCI exhibited an upward trend. During this period, the proportions of mild and general conflicts declined, while the proportions of medium and severe conflicts increased. The results of the spatial autocorrelation analysis indicate that there are spatial interrelationships of land use conflicts within the region. The composite index of spatial conflicts exhibits distinct H-H and L-L aggregation patterns. High-value areas are predominantly located in the cultivated land regions of the northern part of the study area, characterized by frequent human activities, as well as in the intermingled zones of water bodies and unused land in the southwestern part, where significant natural phenomena, such as ice and snow melt, occur. Conversely, low-value areas are primarily found in the grassland regions, which extend in a band across the eastern and western ends of the study area.

(3) The spatial patterns of land use in the urban agglomeration on the northern slopes of the Tianshan Mountains for the years 2030 and 2050 differ across various scenarios. Under the ND scenario, both cultivated land and urban land are projected to increase, while grassland and unused land are expected to decline. Forestland and water bodies are anticipated to remain relatively stable. In the CP scenario, the trends in land area changes are similar to those in the ND scenario; however, the increase in urban land area is less pronounced, with a greater conversion of land to cultivated uses. The EP scenario predicts increases in the areas of grassland, forestland, water bodies, and urban land, while cultivated land and unused land are expected to decrease. This scenario emphasizes the conservation and restoration of forest and grassland, leading

to a significant increase in their areas. Although the urban land area will increase, the growth will be limited due to constraints on urban expansion. Water bodies are expected to be somewhat protected due to an increase in vegetation and restrictions on urban development, resulting in a modest increase in their area.

(4) Under the ND scenario, land use conflict is projected to show a continuous upward trend from 2020 to 2050, whereas under both the CP and EP scenarios, land use conflict is expected to initially rise before declining back to original levels.

Author Contributions: Data curation, Y.M. (Yunfei Ma); Formal analysis, Y.M. (Yunfei Ma); Investigation, Y.M. (Yunfei Ma); Methodology, Y.M. (Yunfei Ma); Software, Y.M. (Yunfei Ma); Supervision, Y.M. (Yusuyunjiang Mamitimin) and A.N.; Visualization, Y.M. (Yunfei Ma); Writing—original draft, Y.M. (Yunfei Ma); Writing—review and editing, Y.M. (Yusuyunjiang Mamitimin) and A.N. All authors have read and agreed to the published version of the manuscript.

Funding: This research was funded by the Natural Sciences Foundation of Xinjiang Uygur Autonomous Region (Grant No.: 2024D01C19).

Institutional Review Board Statement: Not applicable.

Informed Consent Statement: Not applicable.

Data Availability Statement: The original contributions presented in this study are included in the article. Further inquiries can be directed to the corresponding author.

Acknowledgments: We would like to thank the Natural Sciences Foundation of Xinjiang Uygur Autonomous Region for funding this research. We also would like to thank the anonymous reviewers for their constructive comments to improve the quality of this manuscript.

Conflicts of Interest: The authors declare no conflicts of interest.

References

1. Wang, J.; Liu, X. Recognizing and measuring spatial conflict of land use via "risk-effect". *Trans. Chin. Soc. Agric. Eng.* **2022**, *38*, 291–300.
2. Zhou, D.; Xu, J.; Wang, L. Land use spatial conflicts and complexity: A case study of the urban agglomeration around Hangzhou Bay, China. *Geogr. Res.* **2015**, *34*, 1630–1642.
3. Guili, L.I.U.; Fengtian, Y.A.N.; Shuncai, X.U.; Xineng, W.; Jingquan, X.U. The strategic disposition between the conflict and coordination from internal and external space in urban development: Taking Shijiazhuang city as a case. *Geogr. Res.* **2006**, *25*, 701–709.
4. Yao, S.; Guan, C.; Wang, S.; Chen, S. The Research on New Characteristics of Urbani zation and the Strategy of Rigional Space Construction in China. *Adv. Earth Sci.* **2007**, *22*, 271–280.
5. Xu, Y.-X.; Chen, F.; Pu, L.J. A Retrospect and Prospect on Research of Urban Spatial and Land Use Expansion. *Econ. Geogr.* **2007**, *27*, 296–301.
6. Kang, L.; Ma, L.; Liu, Y. Analysis on the Time-spatial Coupling Character of Urbanization and Cultivated Land Resource in China. *Areal Res. Dev.* **2017**, *36*, 87–92.
7. Li, X.J.; Peterson, J.; Liu, G.J.; Qian, L.X. Assessing regional sustainability: The case of land use and land cover change in the middle Yiluo catchment of the Yellow River basin, China. *Appl. Geogr.* **2001**, *21*, 87–106. [CrossRef]
8. Ma, L.; Luo, Q. Spatial-temporal Characteristics and Mechanism of Urbanization and Rural Development Coupling Coordination in China. *Areal Res. Dev.* **2017**, *36*, 45–49, 92.
9. Fan, H.; Liu, W.; Wu, Z. Spatio-temperal Characteristics of Internal Coordination of Intensive Urban Land Use: A Case Study of the Downtown of Wuhan. *Sci. Geogr. Sin.* **2014**, *34*, 696–704.
10. Liu, X.; Feng, Z.; Jiang, L.; Zhang, J. Spatial-Temporal Pattern Analysis of Land Use and Land Cover Change in Xishuangbanna. *Resour. Sci.* **2014**, *36*, 233–244.
11. Zhu, H.; Sun, M. Main progress in the research on land use intensification. *Acta Geogr. Sin.* **2014**, *69*, 1346–1357.
12. Bohua, Y.U.; Changhe, L.V. The Progress and Prospect of Land Use Conflicts. *Prog. Geogr.* **2006**, *25*, 106–115.
13. Yongfang, Y.; Lianqi, Z.J.R.S. The Theory and Diagnostic Methods of Land Use Conflicts. *Resour. Sci.* **2012**, *34*, 1134–1141.
14. Hilson, G. An overview of land use conflicts in mining communities. *Land Use Policy* **2002**, *19*, 65–73. [CrossRef]

15. Zhou Guohua, P.J. The Evolution Characteristics and Influence Effect of Spatial Conflict: A Case Study of Changsha-Zhuzhou-Xiangtan Urban Agglomeration. *Prog. Geogr.* **2012**, *31*, 717–723. [CrossRef]
16. Zou, L.; Liu, Y.; Wang, Y. Research progress and prospect of land-use conflicts in China. *Prog. Geogr.* **2020**, *39*, 298–309. [CrossRef]
17. Campbell, D.J.; Gichohi, H.; Mwangi, A.; Chege, L. Land use conflict in Kajiado District, Kenya. *Land Use Policy* **2000**, *17*, 337–348. [CrossRef]
18. Moore, W.; Lindström, R.; Oregan, V. Land reform, political violence and the economic inequality-political conflict nexus: A longitudinal analysis. *Int. Interact.* **1996**, *21*, 335–363. [CrossRef]
19. Benjaminsen, T.A.; Alinon, K.; Buhaug, H.; Buseth, J.T. Does climate change drive land-use conflicts in the Sahel? *J. Peace Res.* **2012**, *49*, 97–111. [CrossRef]
20. Tudor, C.A.; Ioja, I.C.; Patru-Stupariu, I.; Nita, M.R.; Hersperger, A.M. How successful is the resolution of land-use conflicts? A comparison of cases from Switzerland and Romania. *Appl. Geogr.* **2014**, *47*, 125–136. [CrossRef]
21. Sauer, A. European nature conservation policy: Challenges for local implementation in Germany. In *From Landscape Research to Landscape Planning*; Springer: Dordrecht, The Netherlands, 2005; pp. 173–189.
22. Ioja, C.L.; Nita, M.R.; Vanau, G.O.; Onose, D.A.; Gavrilidis, A.A. Using multi-criteria analysis for the identification of spatial land-use conflicts in the Bucharest Metropolitan Area. *Ecol. Indic.* **2014**, *42*, 112–121. [CrossRef]
23. Valera, C.A.; Valle Junior, R.F.; Varandas, S.G.P.; Sanches Fernandes, L.F.; Pacheco, F.A.L. The role of environmental land use conflicts in soil fertility: A study on the Uberaba River basin, Brazil. *Sci. Total Environ.* **2016**, *562*, 463–473. [CrossRef] [PubMed]
24. Hunsberger, C.; Work, C.; Herre, R. Linking climate change strategies and land conflicts in Cambodia: Evidence from the Greater Aural region. *World Dev.* **2018**, *108*, 309–320. [CrossRef]
25. Shukui, T. Discussion on Classification Scheme of Land Conflict in China. *Chin. J. Agric. Resour. Reg. Plan.* **2008**, *29*, 27–30.
26. Zong, S.; Hu, Y.; Zhang, Y.; Wang, W. Identification of land use conflicts in China's coastal zones: From the perspective of ecological security. *Ocean. Coast. Manag.* **2021**, *213*, 105841. [CrossRef]
27. Xue-Guang, M.A.; Ai-Min, W.; Xiao-Pei, Y.J.H.G. A Study on Land Use Conflicts in the Urban Spatial Reconstruction Process—A Case Study of Guangzhou City. *Hum. Geogr.* **2010**, *3*, 72–77.
28. Wang, Y.; Li, W.; Zeng, X.; Li, P.; Xue, B. The Spatial Multi-scale Mechanism of Land Use Elemental Conflicts in Shenyang Economic Zone. *Econ. Geogr.* **2022**, *42*, 231–239.
29. Lu, S.-y.; Zhang, J.-y.; Wu, Z.-p. Study on the Spatial Conflict of Land Use in Jinghe County Oasis. *J. Ecol. Rural Environ.* **2022**, *38*, 428–436. [CrossRef]
30. Dai, Z.; Yang, C.; Xin, G.; Wei, Y.; Xiong, X. Evaluation of Land Use Conflicts in Hilly and Mountainous Areas and Optimization of Their Control. *J. Southwest Univ.* **2019**, *41*, 82–91.
31. Liao, L.; Dai, W.; Chen, J.; Huang, W.; Jiang, F.; Hu, Q. Spatial conflict between ecological-production-living spaces on Pingtan Island during rapid urbanization. *Resour. Sci.* **2017**, *39*, 1823–1833.
32. Liu, Y.; Chen, B. The study framework of land use/cover change based on sustainable development in China. *Geogr. Res.* **2002**, *21*, 324–330.
33. Tu, X.S.; Pu, L.J. Spatio-temporal pattern of land use change and its eco-environmental response in Suzhou-Wuxi-Changzhou Region. *Geogr. Res.* **2008**, *27*, 583–593.
34. Xie, H.; Li, B. Driving forces analysis of land-use pattern changes based on logistic regression model in the farming-pastoral zone: A case study of Ongiud Banner, Inner Mongolia. *Geogr. Res.* **2008**, *27*, 294–304.
35. Shi, M.; Jiang, L.; Fu, Y. Study on Prediction Methods for the Fault State of Rotating Machinery Based on Dynamic Grey Model and Metabolism Grey Model. *Wirel. Pers. Commun.* **2018**, *102*, 3615–3627. [CrossRef]
36. Tobler, W.R. A Computer Movie Simulating Urban Growth in the Detroit Region. *Econ. Geogr.* **1970**, *46*, 234–240. [CrossRef]
37. Zhao, T.; Chen, W.; Li, F.; Luo, X. Dynamic Simulation Analysis of Land Use Ecological Effects Based on CLUE-S and Ecological Sensitivity Analysis. *Acta Agric. Univ. Jiangxiensis* **2013**, *35*, 1296–1302.
38. Huang, J.; Lin, H.; Qi, X. A literature review on optimization of spatial development pattern based on ecological-production-living space. *Prog. Geogr.* **2017**, *36*, 378–391.
39. Liu, X.; Liang, X.; Li, X.; Xu, X.; Ou, J.; Chen, Y.; Li, S.; Wang, S.; Pei, F. A future land use simulation model (FLUS) for simulating multiple land use scenarios by coupling human and natural effects. *Landsc. Urban Plan.* **2017**, *168*, 94–116. [CrossRef]
40. Luo, M.; Peng, S. Simulation of land use change in central Yunnan based on FLUS model. In Proceedings of the 2020 IEEE International Conference on Information Technology, Big Data and Artificial Intelligence (ICIBA), Chongqing, China, 6–8 November 2020; pp. 1375–1378.
41. Yuan, Y.; Shi, P.; Liu, Y.; Xie, F. A study on the pattern of land cover during rapid urbanization: Shenzhen City as a case study. *Acta Ecol. Sin.* **2003**, *23*, 1832–1840.
42. Zhao, L.; Liu, X.; Liu, P.; Chen, G.; He, J. Urban Expansion Simulation and Early Warning based on Geospatial Partition and FLUS Model. *J. Geo-Inf. Sci.* **2020**, *22*, 517–530.

43. Wang, W.; Chen, H.; Cao, S.; Wang, B. Analysis of Urban Dual-Carbon Targets and Countermeasures Based on GeoSOS-FLUS Simulation–A Case of Hangzhou City, Zhejiang Province. In *Proceedings of the 2022 International Conference on Green Building, Civil Engineering and Smart City*; Springer: Singapore, 2023; pp. 32–43.
44. Shao, X.; Jing, C.; Qi, J.; Jiang, J.; Liu, Q.; Cai, X. Impacts of land use and planning on island ecosystem service values: A case study of Dinghai District on Zhoushan Archipelago, China. *Ecol. Process.* **2017**, *6*, 27. [CrossRef]
45. Liang, H.; Alimujiang, K.; Zhao, H.; Zhao, Y. Analysis of the spatial and temporal differences in surface temperature and the contribution of surface coverage in the urban agglomeration on the northern slope of the Tianshan Mountains. *Arid Zone Res.* **2022**, *39*, 388–399.
46. Duan, Z.; Liu, Y.; Wang, J.; Wen, K. Urban niche metrics: A case of the urban agglomeration in Northern Slope of Tianshan Mountains. *Arid Land Geogr.* **2013**, *36*, 1153–1161.
47. Liu, Y.; Li, L.; Ju, C. Spatio-temporal Evolution of Land Use and Ecological Service Value in Urban Agglomeration on Northern Slope of Tianshan Mountains. *Bull. Soil Water Conserv.* **2020**, *40*, 312–320.
48. Shang, H.; Wang, W.; Dai, Z.; Duan, L.; Zhao, Y.; Zhang, J. An ecology-oriented exploitation mode of groundwater resources in the northern Tianshan Mountains, China. *J. Hydrol.* **2016**, *543*, 386–394. [CrossRef]
49. Fang, C.; Gao, Q.; Zhang, X.; Cheng, W. Spatiotemporal characteristics of the expansion of an urban agglomeration and its effect on the eco-environment: Case study on the northern slope of the Tianshan Mountains. *Sci. China Earth Sci.* **2019**, *62*, 1461–1472. [CrossRef]
50. Kucsicsa, G.; Popovici, E.-A.; Balteanu, D.; Grigorescu, I.; Dumitrascu, M.; Mitrica, B. Future land use/cover changes in Romania: Regional simulations based on CLUE-S model and CORINE land cover database. *Landsc. Ecol. Eng.* **2019**, *15*, 75–90. [CrossRef]
51. Peng, J.; Zhou, G.; Tang, C.; He, Y. The Analysis of Spatial Conflict Measurement in Fast Urbanization Region Based on Ecological SecurityA Case Study of Changsha-Zhuzhou-Xiangtan Urban Agglomeration. *J. Nat. Resour.* **2012**, *27*, 1507–1519.
52. Chen, Z.; Feng, X.; Hong, Z.; Li, Y. Calculation and Analysis of Spatial Conflicts in Land Use of Nanchang City. *Areal Res. Dev.* **2020**, *39*, 150–155.
53. Meng, J.; Jiang, S.; Laba, Z.; Zhang, W. The Spatial and Temporal Analysis of Land Use Conflict in the Middle Reaches of the Heihe River Based on Landscape Pattern. *Sci. Geogr. Sin.* **2020**, *40*, 1553–1562.
54. Ma, B.; Feng, X.; Li, Y.; Hong, Z.; Chen, Z.A. Research on spatial conflict calculation and zoning optimization of land use in Nanchang City from the perspective of "three living spaces". *J World Reg. Stud.* **2021**, *30*, 533–545. [CrossRef]
55. Qiu, G.; Niu, Q.; Wu, Z.; Guo, S.; Qin, L.; Wang, Y. Spatial Evaluate and Heterogeneity Analysis of Land Use Conflict in Su-Xi-Chang Urban Agglomeration. *Res. Soil Water Conserv.* **2022**, *29*, 400–406,414.
56. Dong, G.; Sun, Z.; Li, W.; Wang, K.; Yuan, C. Identification of Potential Land Use Conflicts in Shandong Province: A New Framework. *Land* **2024**, *13*, 1203. [CrossRef]
57. Ni, C.; He, W.; Yao, Y. Assessment of cultivated land use change in Guilin using the GeoSOS-FLUS model. *Bull. Surv. Mapp.* **2024**, *5*, 35–40.
58. Yang, C.; Wu, G.; Chen, J.; Li, Q.; Ding, K.; Wang, G.; Zhang, C. Simulating and forecasting spatio-temporal characteristic of land-use/cover change with numerical model and remote sensing: A case study in Fuxian Lake Basin, China. *Eur. J. Remote Sens.* **2019**, *52*, 374–384. [CrossRef]
59. Li, H.; Fang, C.; Xia, Y.; Liu, Z.; Wang, W. Multi-Scenario Simulation of Production-Living-Ecological Space in the Poyang Lake Area Based on Remote Sensing and RF-Markov-FLUS Model. *Remote Sens.* **2022**, *14*, 2830. [CrossRef]
60. Xiang, S.; Wang, Y.; Deng, H.; Yang, C.; Wang, Z.; Gao, M. Response and multi-scenario prediction of carbon storage to land use/cover change in the main urban area of Chongqing, China. *Ecol. Indic.* **2022**, *142*, 109205. [CrossRef]
61. Yang, X.; Zheng, X.-Q.; Chen, R. A land use change model: Integrating landscape pattern indexes and Markov-CA. *Ecol. Model.* **2014**, *283*, 1–7. [CrossRef]
62. Song, Q.; Hu, B.; Peng, J.; Bourennane, H.; Biswas, A.; Opitz, T.; Shi, Z. Spatio-temporal variation and dynamic scenario simulation of ecological risk in a typical artificial oasis in northwestern China. *J. Clean. Prod.* **2022**, *369*, 133302. [CrossRef]
63. Huang, K.; Dai, W.; Huang, W.; Ou, H.; Hu, H. Impacts of Land Use Change Evaluation on Habitat Quality Based on CA-Markov and InVEST Models Taking Fuzhou New District of Fujian Province as an Example. *Bull. Soil Water Conserv.* **2019**, *39*, 155–162.
64. Sang, L.; Zhang, C.; Yang, J.; Zhu, D.; Yun, W. Simulation of land use spatial pattern of towns and villages based on CA-Markov model. *Math. Comput. Model.* **2011**, *54*, 938–943. [CrossRef]
65. Chen, L.; Cai, H.; Zhang, T.; Zhang, X.; Zeng, H. Land use multi-scenario simulation analysis of Rao River Basin based on Markov-FLUS model. *Acta Ecol. Sin.* **2022**, *42*, 3947–3958.
66. Pontius, R.G., Jr.; Millones, M. Death to Kappa: Birth of quantity disagreement and allocation disagreement for accuracy assessment. *Int. J. Remote Sens.* **2011**, *32*, 4407–4429. [CrossRef]
67. Pinto, N.; Antunes, A.P.; Roca, J. Applicability and calibration of an irregular cellular automata model for land use change. *Comput. Environ. Urban Syst.* **2017**, *65*, 93–102. [CrossRef]

68. He, J.; Xia, L.; Yao, Y.; Ye, H.; Zhang, J. Mining transition rules of cellular automata for simulating urban expansion by using the deep learning techniques. *Int. J. Geogr. Inf. Sci.* **2018**, *32*, 2076–2097. [CrossRef]
69. Yuan, X.; Zhou, J.; Hu, B.; Gao, Q. Multi-scenario simulation and prediction of ecological-productive-living spaces in Guangdong-Hong Kong-Macao Greater Bay Area based on FLUS model. *Sci. Geogr. Sin.* **2023**, *43*, 564–574.
70. Wang, X.; Yao, Y.; Ren, S.; Shi, X. A Coupled FLUS and Markov Approach to Simulate the Spatial Pattern of Land Use in Rapidly Developing Cities. *J. Geo-Inf. Sci.* **2022**, *24*, 100–113.
71. Zeng, H.; Gao, L.; Xia, J. Dynamic analysis of urban landscape using a modified conversion matrix method:A case study in Nanchang City. *Acta Ecol. Sin.* **2003**, *23*, 2201–2209.
72. Shi, N.; Zhao, H.; Ren, T.; Qi, R. Construction research on the whole-process supervision and management mechanism of high-standard farmland. *J. China Agric. Univ.* **2022**, *27*, 173–185.
73. Chen, L.; Li, X.; Fu, B.; Xiao, D.; Zhao, W. Development history and future research priorities of landscape ecology in China. *Acta Ecol. Sin.* **2014**, *34*, 3129–3141.
74. HuaLin, X.I.E. Regional eco-risk analysis of based on landscape structure and spatial statistics. *Acta Ecol. Sin.* **2008**, *28*, 5020–5026.
75. Chen, D.; Zhou, X.; Hu, F.; Pei, Y.; Hu, Y.; Luo, W. Analysis of Spatial and Tempoal Changes in Land Use Conflicts in Guiyang City in the Last 30 Years. *Res. Soil Water Conserv.* **2023**, *30*, 337–344,356.
76. Li, X.; Yang, G.; Zhou, Y.; Li, B.; Zhang, X. Evaluation of urban landscape ecological security in karst areas based on 3S technologies: An example of Guiyang City. *Carsologica Sin.* **2016**, *35*, 340–348.
77. De, Z.; Jian-Chun, X.U.; Li, W. Process of Land Use Conflict Research in China During the Past Fifteen Years. *China Land Sci.* **2015**, *29*, 21–29.
78. Tian, L.; Lyu, S.; Wu, Z.; Wang, J.; Shi, X. Changes and spatial conflict measurement of land use in Urumqi City. *Remote Sens. Nat. Resour.* **2023**, *35*, 282–291.
79. Ran, D.; Zhang, Z.; Jing, Y. A Study on the Spatial-Temporal Evolution and Driving Factors of Non-Grain Production in China's Major Grain-Producing Provinces. *Int. J. Environ. Res. Public Health* **2022**, *19*, 16630. [CrossRef]

Disclaimer/Publisher's Note: The statements, opinions and data contained in all publications are solely those of the individual author(s) and contributor(s) and not of MDPI and/or the editor(s). MDPI and/or the editor(s) disclaim responsibility for any injury to people or property resulting from any ideas, methods, instructions or products referred to in the content.